Supporting Information

# A dinuclear porphyrin-macrocycle as synergistic catalyst for the hydrogen evolution reaction

Julia Jökel,[†a] Fabian Schwer,[†b] Max von Delius*[b] and Ulf-Peter Apfel*[ac]

[a] Inorganic Chemistry I, Ruhr-University Bochum, Universitätsstr. 150, 44801 Bochum, Germany. E-mail: ulf.apfel@rub.de or ulf-peter.apfel@umsicht.fraunhofer.de.

[b] Institute of Organic Chemistry, University of Ulm, Albert-Einstein-Allee 11, 89081 Ulm, Germany. E-mail: max.vondelius@uni-ulm.de .

[c] Fraunhofer UMSICHT, Osterfelder Str. 3, 46047 Oberhausen, Germany.

[†] These authors contributed equally.

## Table of Contents

# 1. General Experimental Section

### Reagents

All commercially available chemicals were purchased from Sigma Aldrich, TCI Deutschland GmbH, VWR International, Fischer scientific, Carl Roth GmbH & Co., Acros Organics and Alfa Aesar. All of them were used without further purification. Anhydrous solvents were dried prior to use in a MBraun SPS-800 instrument.

### NMR

NMR spectra were recorded on a Bruker Avance 400 spectrometer ($^{1}$H: 400 MHz, $^{13}$C: 100 MHz) or a Bruker AMX 500 spectrometer at 293 K. Chemical shifts (δ) are reported in ppm using residual solvent protons ($^{1}$H NMR: $\delta_H$ = 7.26 for $CDCl_3$;; $^{13}$C NMR: $\delta_C$ = 77.16 for $CDCl_3$) as internal standard. The splitting patterns are designated as follows: s (singlet), d (doublet), t (triplet), and m (multiplet). Coupling constants *J* relate to proton-proton couplings.

### Mass Spectrometry

High resolution MALDI mass spectra were recorded on a Bruker SolariX using *trans*-2-[3-(4-*tert*-butylphenyl)-2-methyl-2-propenylidene]malononitrile (DCTB) as matrix. High resolution ESI mass spectra were recorded on Bruker SolariX (Hybrid 7T FT-ICR).

### Column and Thin Layer Chromatography

The normal-phase flash column chromatography was performed using silica 60 with a particle size of 0.04 – 0.063 mm from Macherey-Nagel. Thin layer chromatography was performed using TLC sheets with a particle size of 60 µm. Spots were detected using UV light of 254 nm wavelength.

## Melting Points

Melting points were determined using a Büchi Melting Point B-545.

## UV-vis Spectroscopy

UV-vis spectra were recorded using a Fisher NanoDrop OneC with a quartz cuvette in DCM solution

## Electrochemistry

The electrochemical studies were performed using a PalmSens3 or a PalmSens4 potentiostat in a standard three-electrode setup. A glassy carbon electrode was used as working electrode (WE), an Ag wire as pseudo-reference electrode (PRE) and a Pt wire as counter electrode (CE). The working electrode was prepared by successive polishing with 1.0 and 0.3 µm sandpaper and subsequent sonication in DCM for 10 min. Tetrabutylammonium hexafluorophosphate ([$^{n}$Bu$_4$N][PF$_6$], 0.1 M) was used as electrolyte in all electrochemical measurements. Prior to each experiment, the electrochemical cell was degassed with Ar for 10 min. and an Ar atmosphere was maintained throughout the measurement. All cyclic voltammograms were recorded at a scan rate of 100 mV $s^{-1}$ and after every experiment all pseudo-referenced potentials were referenced against the ferrocene/ferrocenium couple ($Fc/Fc^{+}$). Controlled potential coulometries (CPC) were performed at defined potentials under otherwise identical conditions as reported above. The electrochemical cell for long-term electrolysis contained 1 mL electrolyte and a headspace of 11 mL.

## GCMS

Quantification of the headspace gas composition and liquid phase composition of the electrochemical cell was performed using a Shimadzu GCMS-QP2020 system equipped with two capillary columns and a MS detector. Gas phase separation was performed *via* hand injection using a Carboxen 1010 PLOT fused silica capillary GC column (L x I.D. 30 m x 0.32 mm, average thickness 15 µm) and liquid phase separation was performed *via* headspace analysis using a SH-Rtx-200ms fused silica

capillary GC column (L x I.D. 30 m x 0.25 mm, average thickness 1 µm). Helium was used as carrier gas. The following gaseous and liquid products/components were assayed *via* the GCMS system: $H_2$, $O_2$, $N_2$, CO, $CH_4$, $C_2H_4$, $C_2H_6$, methanol, ethanol, propanol, formate/formic acid, acetate/acetic acid, propionate/propionic acid, acetaldehyde and propionaldehyde.

**Spectroelectrochemical UV-vis Spectroscopy**

Spectroelectrochemcial experiments were performed in a SEC-2F Spectro-electrochemical flow cell from ALS Co., Ltd attached to a UV-1900i spectrophotometer from Shimadzu via optical fibres. The flow cell was equipped with a standard three-electrode set-up containing a glassy carbon electrode as working electrode (WE), an Ag wire as pseudo-reference electrode (PRE) and a Pt wire as counter electrode (CE). Tetrabutylammonium hexafluorophosphate ([$^n$Bu$_4$N][PF$_6$], 0.1 M) was used as electrolyte during the electrochemical measurements. Controlled potential coulometries (CPC) were performed at a defined potential for 30 min. while UV-vis spectra were recorded every 2 min.

**DFT Calculations**

Relaxed geometries were obtained from density-functional theory (DFT) calculations. The calculations were carried out with Gaussian quantum chemistry software package (Gaussian ® 09 system[1]) on the high-performance computer system 'bwForCluster Chemistry' of the state Baden-Württemberg. Electronic properties were determined using the B3LYP functional and the 6-31G(d) basis set. The 2-butyloctyloxy chains were replaced by methoxy groups to reduce the complexity and computational cost. In the geometry optimizations, structures were assumed to be relaxed when a force convergence threshold of 4.5 meV/A was reached.

## 2. Overview on Synthesis

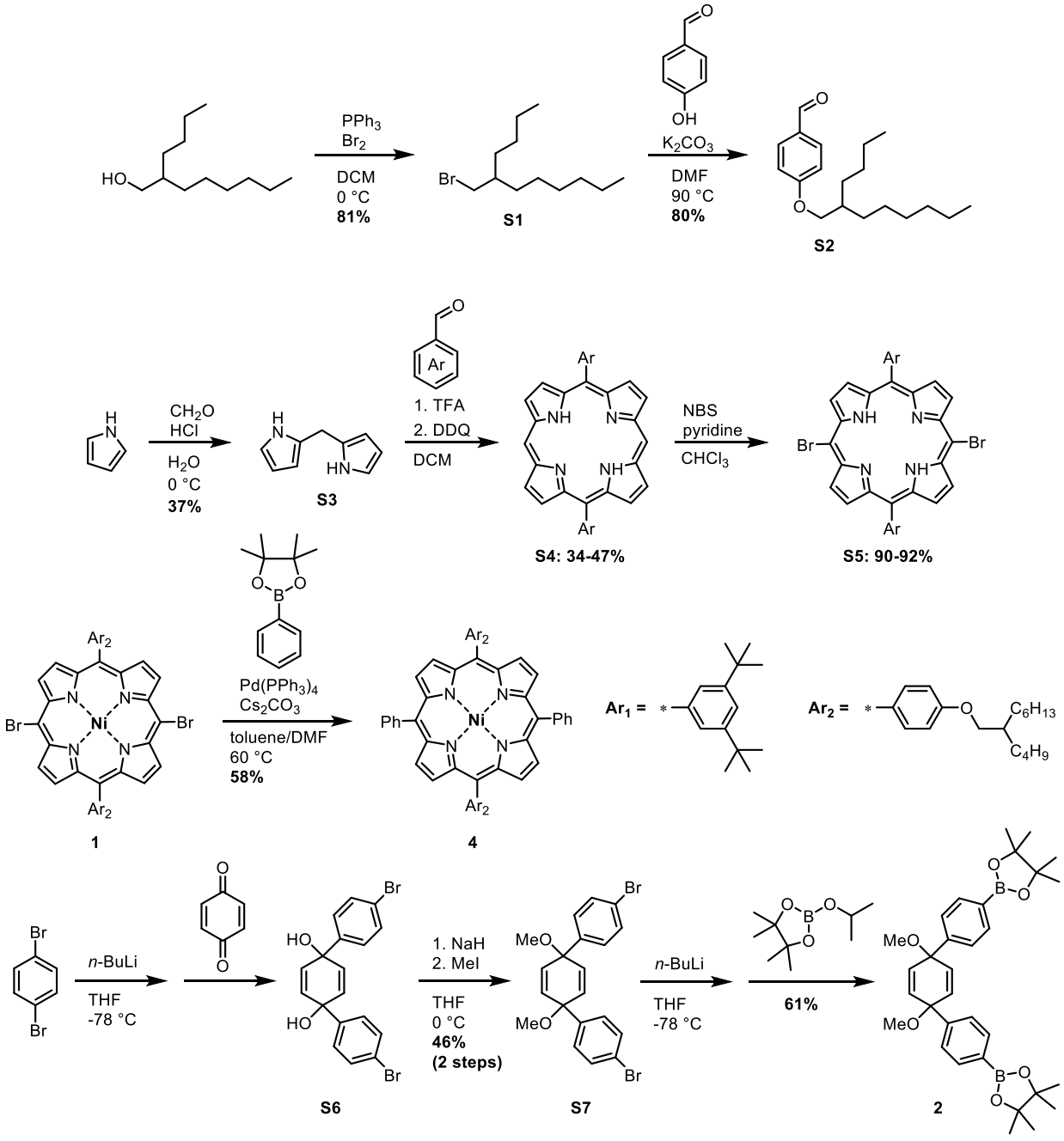


**Figure S1**: Overview on synthesis.

## 3. Macrocyclization of the Porphyrins

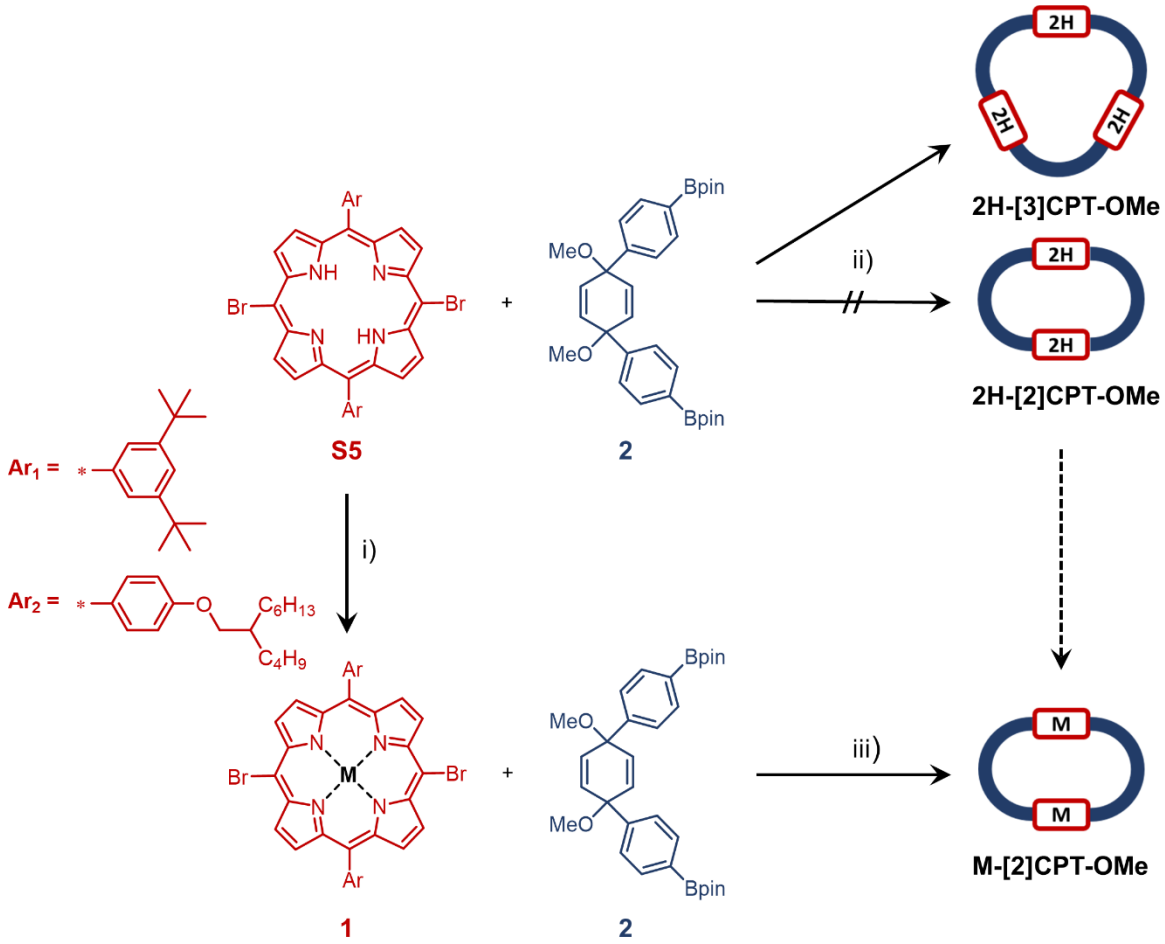


**Figure S2**: Overview on the macrocyclization strategy *via* Suzuki cross coupling. Reaction conditions: i) Co: $Co(OAc)_2$, toluene, reflux, 84-89%, Ni: $Ni(OAc)_2*4H_2O$, DMF, reflux 82%. ii) Co: $Pd(PPh_3)_4$, $Cs_2CO_3$, toluene, 125°C. iii) Co/Ni: $Pd(PPh_3)_4$, $Cs_2CO_3$, pyrazine, toluene, 125°C, 8% (Ni).

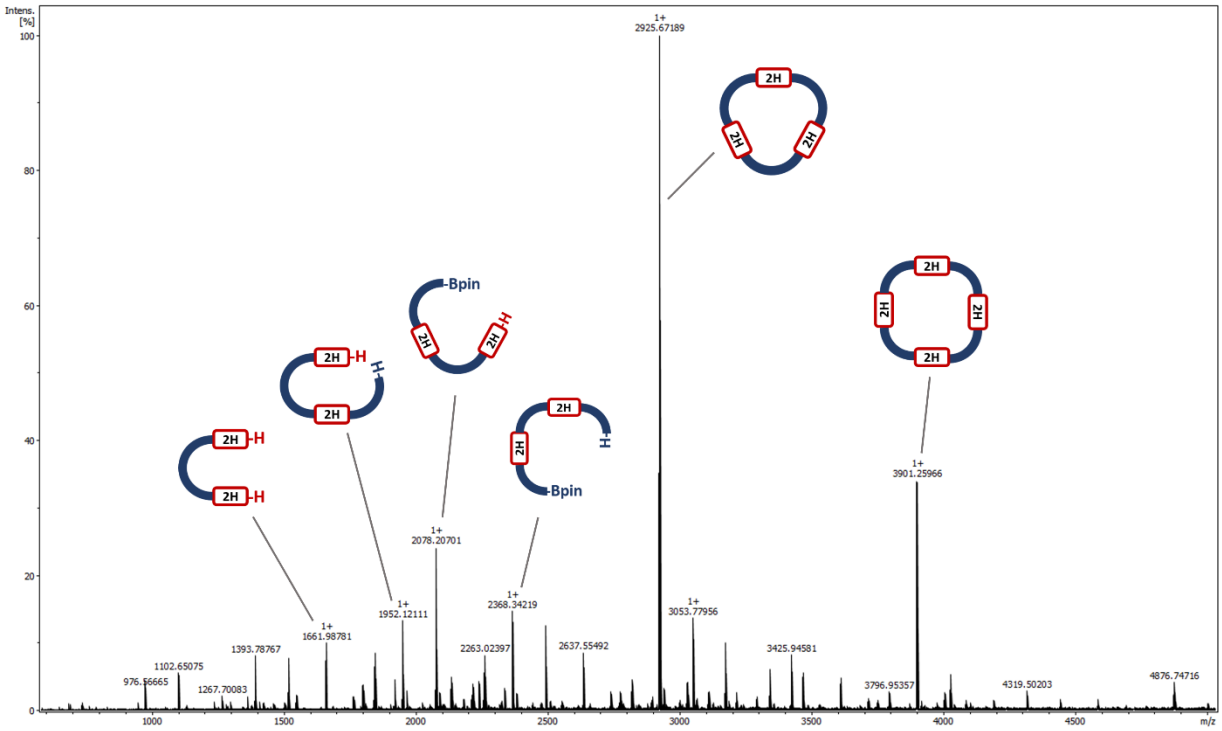


**Figure S3**: HRMS (MALDI, matrix: DCTB) of the Suzuki cross-coupling of the free base porphyrin **S5-Ar$_1$** and the terphenyl linker **2**.

**Conclusion:** In case of the free-base porphyrin, it seems that with the crucial ring-closing step for the formation of the smallest macrocycle is unfavourable and therefore only linear coupling products are observed in the expected mass range.

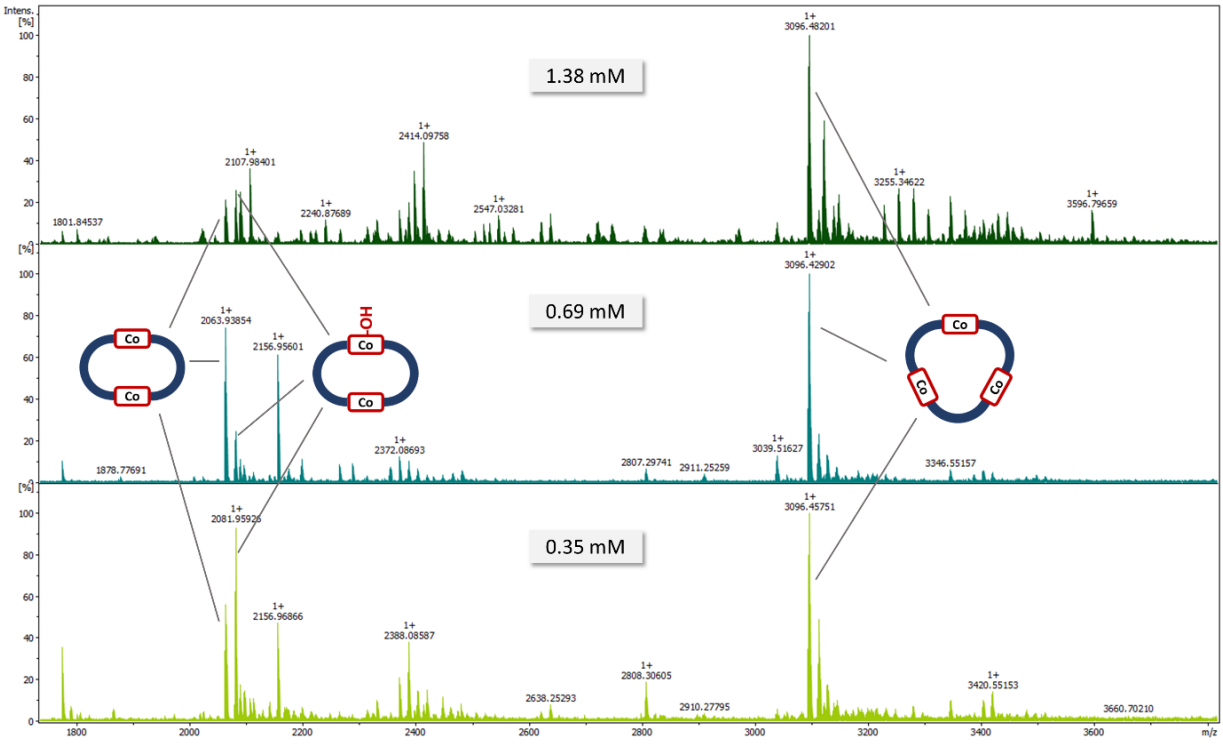


**Figure S4**: HRMS (MALDI, matrix: DCTB) of the Suzuki cross-coupling of cobalt porphyrin **Co-1-Ar$_1$** and the terphenyl linker **2** with pyridine as template and different concentrations of the building blocks in toluene. *m/z* = 2064 [M$^+$] and *m/z* = 2081 [MOH$^+$] refer to **Co-[2]CPT-OMe** and *m/z* = 3096 [M$^+$] to **Co-[2]CPT-OMe**.

**Conclusion:** In case of the Co-porphyrin, the intramolecular ring-closing is preferred over further linear coupling at lower concentrations and therefore the formation of smaller macrocycles is favoured compared to larger macrocycles and linear side products.

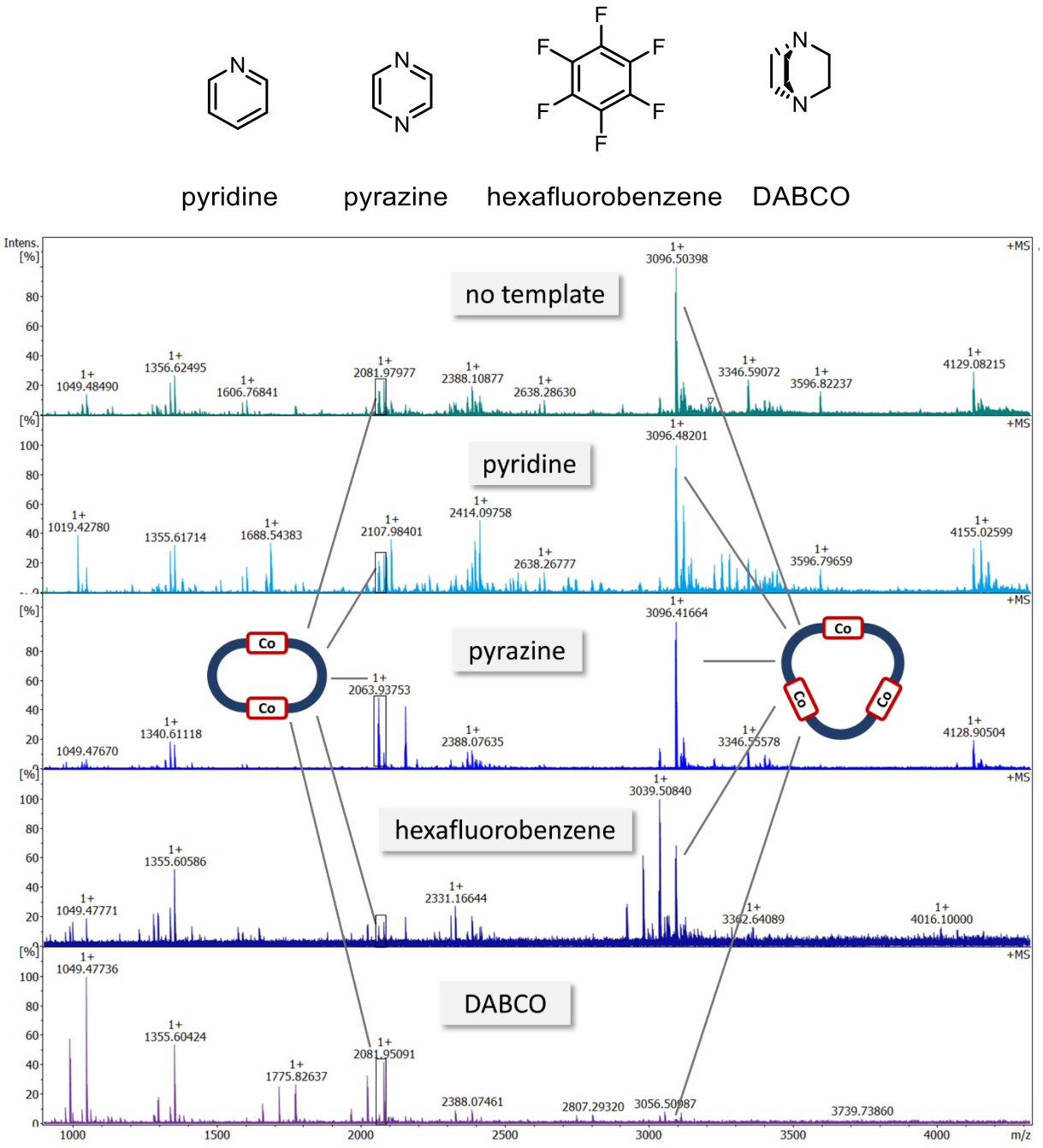


**Figure S5**: HRMS (MALDI, matrix: DCTB) of the Suzuki cross-coupling of cobalt porphyrin **Co-1-Ar$_1$** and the terphenyl linker **2** with different templates and a concentration of 0.69 mM in toluene of the building blocks. *m/z* = 2064 [M$^+$] and *m/z* = 2081 [MOH$^+$] refer to **Co-[2]CPT-OMe** and *m/z* = 3096 [M$^+$] to **Co-[3]CPT-OMe**.

**Conclusion:** This systematic study of various potential templates indicates that, contrary to our previous assumption,[2] a π-π template effect is probably not in operation. We believe that it is more likely that the template effect is resulting from dative bonds between a nitrogen atom and the metal center of the porphyrin. This assumption is based especially on the MS spectrum resulting from the reaction with

DABCO, which favours the formation of **Co-[2]CPT-OMe**, even though it does not have a π-system. Moreover, hexafluorobenzene should be a suitable π-π template, but it fails to produce the desired product. Finally, a dative template effect cannot be used to favour the free-base porphyrin macrocycle, which indeed was not obtained.

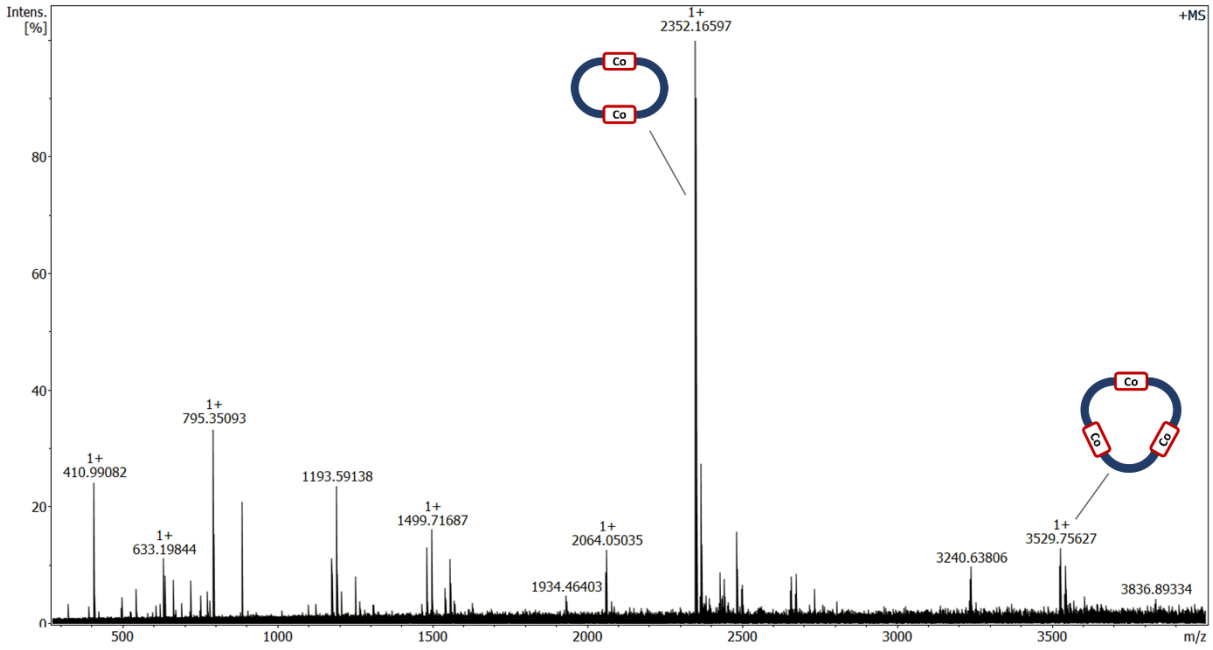


**Figure S6**: HRMS (MALDI, matrix: DCTB) of the Suzuki cross-coupling of cobalt porphyrin **Co-1-Ar$_2$** and the terphenyl linker **2** with pyrazine as template and a concentration of 0.35 mM in toluene.

# 4. Synthetic Procedures and Characterisation Data

**Synthesis of 5-(bromomethyl)undecane (S1)**

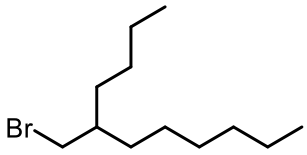


Synthesized according to a literature procedure.[3] Triphenylphosphine (9.02 g, 34.3 mmol, 1.3 equiv) was dissolved in DCM (100 mL) and cooled down to 0 °C. Elemental bromine (1.9 mL, 73.4 mmol, 2.7 equiv) was added dropwise followed by the dropwise addition of 2-butyloctanol (6.0 mL, 26.8 mmol, 1.0 equiv) in pyridine (7.3 mL, 90.4 mmol, 3.4 equiv). The reaction was stirred for a further hour at 0 °C and then allowed to warm up and stirred again for one hour at room temperature. The reaction was quenched with a $K_2CO_3$ solution. The organic layer was washed with water dried over $MgSO_4$ and concentrated under reduced pressure. The crude product was filtered over silica with petroleum ether as eluent to yield compound **S1** as colourless oil (5.38 g, 21.6 mmol, 81%)

**$^1$H NMR** (400 MHz, $CDCl_3$): δ = 3.45 (d, $^3J$ = 4.8 Hz, 2H, Br-C$H_2$), 1.58 (m, 1H, C$H$), 1.42 – 1.22 (m, 16H, (C$H_2$)$_n$), 0.89 (m, 6H, C$H_3$) ppm.

**Synthesis of 4-((2-butyloctyl)oxy)benzaldehyde (S2)**

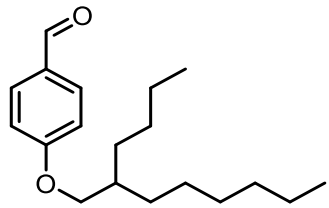

Synthesized according to a literature procedure.[4] 4-Hydroxybenzaldehyde (1.48 g, 12.1 mmol, 1.0 equiv) and $K_2CO_3$ (1.67 g, 12.1 mmol, 1.0 equiv) were dissolved in DMF (26 mL). The mixture was heated to 90 °C and a solution of compound **S1** (3.00 g, 12.1 mmol) in DMF (13 mL) was added dropwise. The mixture was stirred at 90 °C for 5 h and then poured into water. After layer separation the organic layer was washed with 5% aqueous NaOH solution and brine. The combined organic layers were dried over $Mg_2SO_4$ and concentrated under reduced pressure to yield compound **S2** as slightly yellow oil (2.79 g, 9.62 mmol, 80%).

**$^1$H NMR** (400 MHz, $CDCl_3$): δ = 9.88 (s, 1H, C*H*O), 7.83 (d, $^3J$ = 8.8 Hz, 2H, Ph-*H*), 6.99 (d, $^3J$ = 8.7 Hz, 2H, Ph-*H*), 3.91 (d, $^3J$ = 5.7 Hz, 2H, O-C$H_2$), 1.80 (m, 1H, C*H*), 1.52 - 1.15 (m, 16H, (C$H_2$)$_n$), 1.01 – 0.74 (m, 6H, C$H_3$) ppm.

**$^{13}$C NMR** (101 MHz, $CDCl_3$) δ =190.9, 164.6, 132.1, 129.8, 114.9, 71.4, 38.0, 32.0, 31.4, 31.1, 29.8, 29.2, 26.9, 23.1, 22.8, 14.2, 14.2 ppm.

**HR-MS (APCI)** *m/z* = calc. for $C_{19}H_{30}O_2$: 290.2245; found: 291.2324 [$MH^+$]

**Synthesis of di(1*H*-pyrrol-2-yl)methane (S3)**

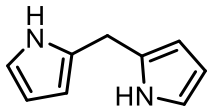

Synthesized according to a literature procedure.[5] Pyrrole (17.0 mL, 245 mmol, 4.1 equiv) was dissolved in water (60 mL) and the solution was degassed via ultrasonication for 30 min and then cooled down to 0 °C. Formaldehyde (4.5 mL, 37% in water, 60 mmol, 1.0 equiv) and HCl (0.2 mL, 35%, 2 mmol, 0.03 equiv) were added dropwise over a period of 15 min and the reaction was stirred for further 2h at 0 °C. The reaction solution was extracted three times with DCM and the combined organic layers were concentrated under reduced pressure. The crude product was purified by distillation (110-120 °C at 0.03 mbar) to yield di(1*H*-pyrrol-2-yl)methane **S3** as colourless solid (3.22 g, 22 mmol, 37%). Since it is prone to slight decomposition at room temperature,[6] compound **S3** was stored in the freezer.

**$^1$H NMR** (400 MHz, $CDCl_3$): δ = 7.93 (bs, 2H, N*H*), 6.71 – 6.62 (m, 2H, α-Py-*H*), 6.15 (m, 2H, ß-Py-*H*), 6.04 (s, 2H, ß-Py-*H*), 4.00 (s, 2H, C$H_2$) ppm.

**$T_m$:** 69.6, lit: 68.9 °C[7]

**Synthesis of 5,15-bis(3,5-di-*tert*-butylphenyl)porphyrin (S4-Ar$_1$)**

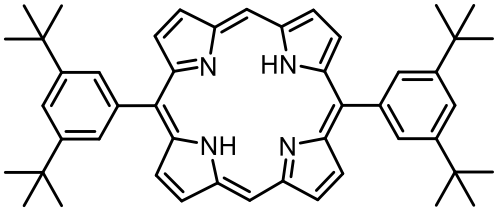


Synthesized according to a literature procedure.[8] 3,5-di-*tert*-butylbenzaldehyde (2.24 g, 10.3 mmol, 1.0 equiv) and di(1*H*-pyrrol-2-yl)methane **S3** ( 1.50 g, 10.3 mmol, 1.0 equiv) were dissolved in DCM (1.50 L) and the solution was degassed via ultrasonication for 20 min. TFA (0.30 mL, 3.9 mmol, 0.38 equiv) was added dropwise and the solution was stirred for 2 h in the dark. DDQ (2.95 g, 13.0 mmol, 1.25 equiv) was then added and the reaction was stirred for a further hour. After TLC indicated only one product, the reaction was quenched with triethylamine and the solvent was removed under reduced pressure. The crude product was purified by column chromatography (DCM/petroleum ether 1:2) to yield porphyrin **S4-Ar$_1$** as red powder (1.67 g, 2.4 mmol, 47%).

**$^1$H NMR** (400 MHz, $CDCl_3$): δ = 10.32 (s, 2H, *meso*-*H*), 9.40 (d, $^{3J}$ = 4.6 Hz, 4H, Py-*H*), 9.14 (d, $^{3J}$ = 4.6 Hz, 4H, Py-*H*), 8.15 (d, $^4J$ = 1.8 Hz, 4H, *o*-Ph-*H*), 7.84 (t, $^4J$ = 1.9 Hz, 2H, *p*-Ph-*H*), 1.58 (s, 36H, C$H_3$) ppm.

**Synthesis of 5,15-bis(4-((2-butyloctyl)oxy)phenyl)porphyrin (S4-Ar$_2$)**

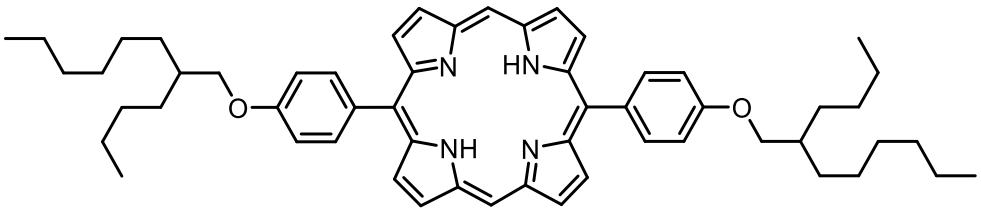


4-((2-butyloctyl)oxy)benzaldehyde **S2** (500 mg, 3.4 mmol, 1.0 equiv) and di(1*H*-pyrrol-2-yl)methane **S3** (994 mg, 3.4 mmol, 1.0 equiv) were dissolved in DCM (750 mL) and the solution was degassed via ultrasonication for 20 min. TFA (0.12 mL, 1.3 mmol, 0.38 equiv) was added dropwise and the solution was stirred for 2 h in the dark. DDQ (964 mg, 4.25 mmol, 1.25 equiv) was then added and the reaction was stirred for a further hour. After TLC indicated only one product, the reaction was quenched with triethylamine and the solvent was removed under reduced pressure. The crude product was purified by column chromatography (DCM/petroleum ether 1:2) to yield porphyrin **S4-Ar$_2$** as purple solid (470 mg, 0.6 mmol, 34%).

**$^1$H NMR** (400 MHz, $CDCl_3$): δ = 10.30 (s, 2H, *meso-H*), 9.39 (d, $^3J$ = 4.6 Hz, 4H, Py-*H*), 9.13 (d, $^3J$ = 4.6 Hz, 4H, Py-*H*), 8.17 (d, $^3J$ = 8.6 Hz, 4H, Ph-*H*), 7.34 (d, $^3J$ = 8.6 Hz, 4H, Ph-*H*), 4.16 (d, $^3J$ = 5.7 Hz, 4H, O-C$H_2$), 2.00 (m, 2H, C*H*), 1.70 – 1.25 (m, 32H, (C$H_2$)$_n$), 1.01 (m, 6H, C$H_3$), 0.98 – 0.93 (m, 6H, C$H_3$) ppm.

**$^{13}$C NMR** (101 MHz, $CDCl_3$) δ =159.5, 147.7, 145.2, 136.0, 133.6, 131.6, 131.2, 119.1, 113.3, 105.3, 71.5, 38.4, 32.1, 31.7, 31.4, 30.0, 29.4, 27.2, 23.4, 22.9, 14.4, 14.4 ppm.

**HR-MS (MALDI)**: *m/z* = calc. for $C_{56}H_{70}N_4O_2$: 830.5498; found: 830.5481 [$M^+$].

**Synthesis of 5,15-dibromo-10,20-bis(3,5-di-*tert*-butylphenyl)porphyrin (S5-Ar$_1$)**

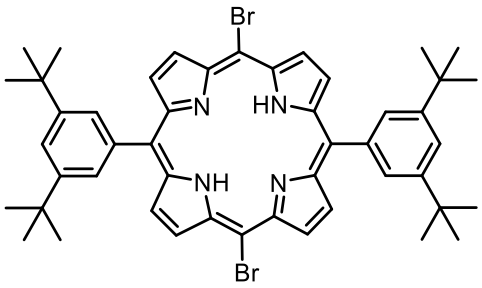


Synthesized according to a literature procedure.[9] Porphyrin **S4-Ar$_1$** (800 mg, 1.16 mmol, 1.0 equiv) was dissolved in chloroform (100 mL). Pyridine (0.3 mL, 3.48 mmol, 3.0 equiv) was added followed by the addition of NBS (477 mg, 2.68 mmol, 2.3 equiv) in portions. After stirring for 30 min in the dark, TLC indicated only one product and the reaction was quenched with acetone. The solvent was removed under reduced pressure and the residue was washed with methanol to yield porphyrin **S5-Ar$_1$** as red powder (903 mg, 10.7 mmol, 92%).

**$^1$H NMR** (400 MHz, $CDCl_3$): δ =9.63 (d, $^3J$ = 4.8 Hz, 4H, Py-*H*), 8.89 (d, $^3J$ = 4.8 Hz, 4H, Py-*H*), 8.03 (d, $^4J$ = 1.8 Hz, 4H, *o*-Ph-*H*), 7.83 (t, $^4J$ = 1.8 Hz, 2H, *p*-Ph-*H*), 1.55 (s, 36H, C$H_3$) ppm.

**UV-Vis** (DCM) $\lambda_{max}$: 423, 523, 558, 603, 659 nm.

**Synthesis of 5,15-dibromo-10,20-bis(4-((2-butyloctyl)oxy)phenyl)porphyrin (S5-Ar$_2$)**

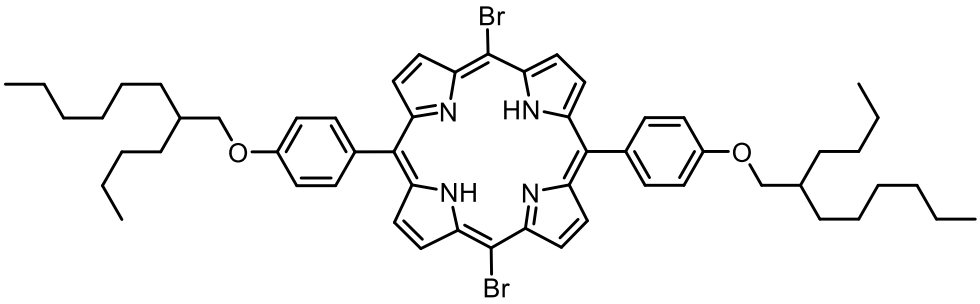


Porphyrin **S4-Ar$_2$** (470 mg, 0.57 mmol, 1.0 equiv) was dissolved in chloroform (70 mL). Pyridine (0.14 mL, 1.7 mmol, 3.0 equiv) was added followed by the addition of NBS (231 mg, 1.3 mmol, 2.3 equiv) in portions. After stirring for 1 h in the dark, TLC indicated only one product and the reaction was quenched with acetone. The solvent was removed under reduced pressure and the residue was washed with methanol to yield porphyrin **S5-Ar$_2$** as purple solid (506 mg, 0.51 mmol, 90%).

**$^1$H NMR** (400 MHz, $CDCl_3$): δ = 9.61 (d, $^3J$ = 4.8 Hz, 4H, Py-*H*), 8.88 (d, $^3J$ = 4.8 Hz, 4H, Py-*H*), 8.05 (d, $^3J$ = 8.1 Hz, 4H, Ph-*H*), 7.29 (d, $^3J$ = 8.2 Hz, 4H, Ph-*H*), 4.14 (d, $^3J$ = 5.6 Hz, 4H, O-C$H_2$), 2.03 – 1.95 (m, 2H, C*H*), 1.60-1.70 (m, 4H, C$H_2$), 1.53 – 1.31 (m, 28H, (C$H_2$)$_n$), 1.01 (t, $^3J$ = 6.8 Hz, 6H, C$H_3$), 0.90 (t, $^3J$ = 6.3 Hz 6H, C$H_3$) ppm.

**$^{13}$C NMR** (101 MHz, $CDCl_3$): δ = 159.6, 135.8, 133.5, 121.5, 113.1, 103.8, 71.4, 38.3, 32.1, 31.7, 31.4, 30.0, 29.4, 27.2, 23.3, 22.9, 14.4, 14.4 ppm.[1]

**HR-MS (MALDI)**: *m/z* = calc. for $C_{56}H_{70}N_4O_2$: 988.3689; found: 988.3668 [$M^+$].

**UV-Vis** (DCM) $\lambda_{max}$: 425, 524, 561, 605, 661 nm.

[1] The four pyrrole shifts in the $^{13}$C NMR spectrum are missing due to unknown reasons, but there is no doubt about the identity of this compound, these $^{13}$C NMR signals appear again after the next step

**Synthesis of [5,15-dibromo-10,20-bis(3,5-di-*tert*-butylphenyl)porphyrinato]cobalt(II) (Co-1-Ar$_1$)**

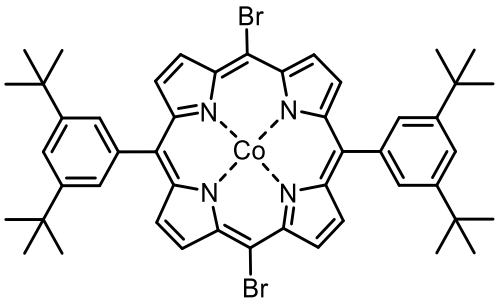


Porphyrin **S5-Ar$_1$** (300 mg, 0.36 mmol, 1.0 equiv) and cobalt(II)acetate (314 mg, 1.8 mmol, 5.0 equiv) were dissolved in toluene (300 mL) and heated under reflux for 1 d. The reaction was concentrated under reduced pressure and the residue was washed with methanol to yield Co(II)porphyrin **Co-1-Ar$_1$** as red powder (288 mg, 0.32 mmol, 89%).

**HR-MS (MALDI)**: *m/z* = calc. for $C_{48}H_{50}Br_2CoN_4$: 901.1714; found: 901.17032 [$M^+$].

**UV-Vis** (DCM) $\lambda_{max}$: 416, 530 nm.

**Synthesis of [5,15-dibromo-10,20-bis(4-((2-butyloctyl)oxy)phenyl)porphyrinato]cobalt(II) (Co-1-Ar$_2$)**

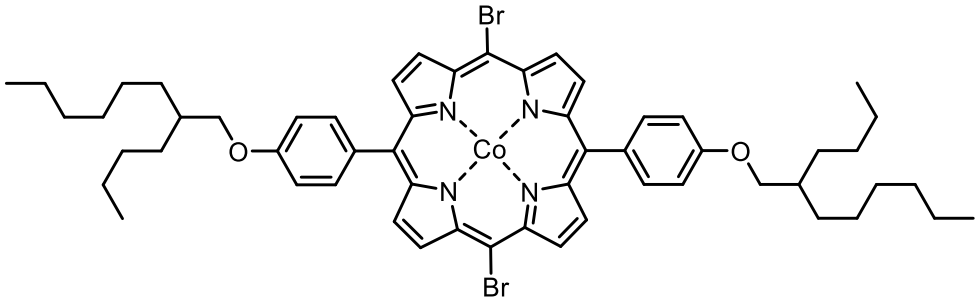


Porphyrin **S5-Ar$_2$** (200 mg, 0.20 mmol, 1.0 equiv) and cobalt(II)acetate (106 mg, 0.60 mmol, 3.0 equiv) were dissolved in toluene (200 mL) and heated under reflux for 4 h. The reaction was concentrated under reduced pressure and the residue was dissolved in DCM and filtered over silica to yield Co(II)porphyrin **Co-1-Ar$_2$** as black solid (176 mg, 0.17 mmol, 84%).

**HR-MS (MALDI)**: *m/z* = calc. for $C_{56}H_{66}Br_2N_4CoO_2$: 1045.2864; found: 1045.2843 [$M^+$].

**UV-Vis** (DCM) $\lambda_{max}$: 417, 537 nm.

**Synthesis of [5,15-dibromo-10,20-bis(4-((2-butyloctyl)oxy)phenyl)porphyrinato]nickel(II) (Ni-1-Ar$_2$)**

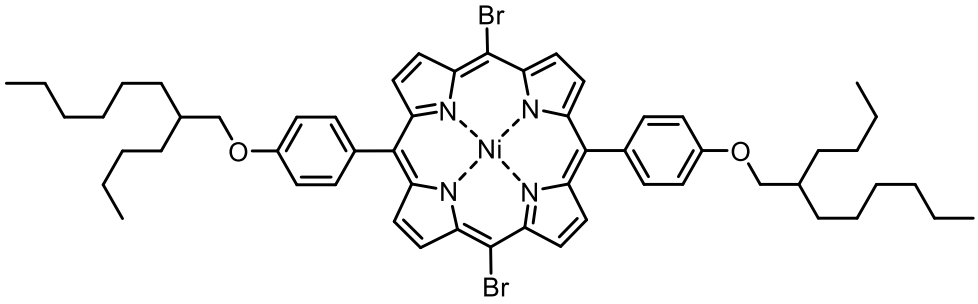


Porphyrin **S5-Ar$_2$** (925 mg, 0.94 mmol, 1.0 equiv) and nickel(II)acetate tetrahydrate (350 mg, 1.40 mmol, 1.5 equiv) were dissolved in DMF (200 mL) and heated under reflux for 5 h. The reaction was concentrated under reduced pressure and the residue was washed with methanol to yield Ni(II)porphyrin **Ni-1-Ar$_2$** as red powder (991 mg, 0.89 mmol, 95%).

**$^1$H NMR** (400 MHz, $CDCl_3$): δ = 9.43 (d, $^3J$ = 5.0 Hz, 4H, Py-*H*), 8.76 (d, $^3J$ = 5.0 Hz, 4H, Py-*H*), 7.83 (d, $^3J$ = 8.3 Hz, 4H, Ph-*H*), 7.21 (d, $^3J$ = 8.3 Hz, 4H, Ph-*H*), 4.08 (d, $^3J$ = 5.6 Hz, 4H, O-C$H_2$), 1.90 – 2.00 (m, 2H, C*H*), 1.53 – 1.31 (m, 32 H, (C$H_2$)$_n$), 0.98 (t, $^3J$ = 6.9 Hz, 6H, C$H_3$), 0.94 (t, $^3J$ = 6.7 Hz 6H, C$H_3$) ppm.

**$^{13}$C NMR** (101 MHz, $CDCl_3$): δ = 159.5, 143.7, 142.7, 134.8, 133.8, 133.5, 132.1, 119.9, 113.2, 102.7, 71.4, 38.3, 32.1, 31.7, 31.4, 30.0, 29.4, 27.1, 23.3, 22.9, 14.4 ppm.

**HR-MS (MALDI)**: *m/z* = calc. for $C_{56}H_{66}Br_2N_4NiO_2$: 1044.2885; found: 1044.2866 [M$^+$].

**UV-Vis** (DCM) $\lambda_{max}$: 422, 538 nm.

**Synthesis of 4,4''-dibromo-[1,1':4',1''-terphenyl]-1',4'-diol (S5)**

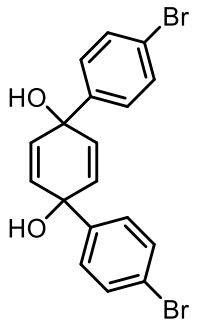


Synthesized according to a literature procedure.[10] Under $N_2$, 1,4-dibromobenzene (4.47 g, 19.0 mmol, 2.05 equiv) was dissolved in anhydrous THF (500 mL). The solution was cooled down to -78 °C and *n*-butyllithium in hexanes (7.8 mL, 2.5 M, 19.4 mmol, 2.1 equiv) was added dropwise. The solution was stirred at -78 °C for 1 h and benzoquinone (1.00 g, 9.25 mmol, 1.0 equiv) was added. The reaction was stirred for further 17 h during which time it was allowed to warm to room temperature. The reaction was quenched with water and the aqueous layer was extracted with diethyl ether. The combined organic layers were dried over $MgSO_4$ and concentrated under reduced pressure to yield the crude product **S5** (2.88 g) as colourless solid, which was used without further purification or characterization for the next step.

**Synthesis of 4,4''-dibromo-1',4'-dimethoxy-1',4'-dihydro-1,1':4',1''-terphenyl (S6)**

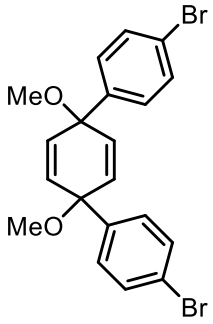


Synthesized according to a literature procedure.[10] Under $N_2$, NaH (1.06 g, 60% in mineral oil, 26.53 mmol, 4.0 equiv) was suspended in anhydrous THF (200 mL) and cooled down to 0 °C. A solution of **S5** (2.88 g, 6.82 mmol, 1.0 equiv) in 5 mL THF was added dropwise and the reaction was stirred for 1 h during which time it was allowed to warm to room temperature. The mixture was re-cooled to 0 °C and MeI (2.06 mL, 33.15 mmol, 5.0 equiv) was added dropwise. The reaction was warmed up to room temperature and stirred for further 15 h. The reaction was quenched with aqueous ammonia solution and diluted with diethyl ether. The aqueous layer was extracted with diethyl ether and the combined organic layers were dried over $MgSO_4$ and concentrated under reduced pressure. Column chromatography (petroleum ether/ EtOAc 19:1 → 9:1) yielded compound **S6** as colourless solid (1.93 g, 4.28 mmol, 46% over two steps).

**$^1$H NMR** (400 MHz, $CDCl_3$,): δ = 7.43 (d, $^3J$ = 8.6 Hz, 4H, Ph-*H*), 7.24 (d, $^3J$ = 8.6 Hz, 4H, Ph-*H*), 6.07 (s, 4H, alkene-*H*), 3.41 (s, 6H, O-C$H_3$) ppm.

**M.p.:** 134 °C, lit: 134.0 – 135.7 °C[10]

**Synthesis of 2,2'-(1',4'-dimethoxy-1',4'-dihydro-[1,1':4',1''-terphenyl]-4,4''-diyl)bis(4,4,5,5-tetramethyl-1,3,2-dioxaborolane) (2)**

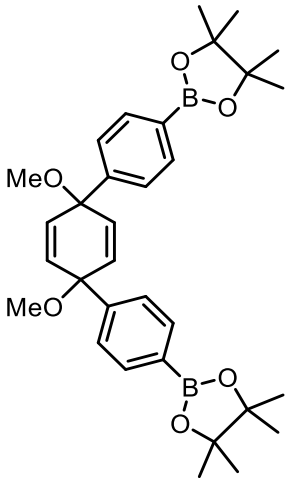


Synthesized according to a literature procedure.[10] Under $N_2$, compound **S6** (0.90 g, 2.00 mmol, 1.0 equiv) was dissolved in anhydrous THF (80 mL) and the solution was cooled down to -78 °C. *n*-butyllithium in hexanes (2.0 mL, 2.5 M, 5.00 mmol, 2.5 equiv) was added dropwise and the reaction was stirred for 20 min during which time it was allowed to warm to -60 °C. 2-Isopropoxy-4,4,5,5-tetramethyl-1,3,2-dioxaborolane (1.22 mL, 6.00 mmol, 3.0 equiv) was added dropwise and the reaction was stirred for further 30 min. The reaction was quenched with water and diluted with diethyl ether. The aqueous layer was extracted with diethyl ether and the combined organic layers were dried over $MgSO_4$ and concentrated under reduced pressure. The residue was washed with methanol to yield the pure boronic ester **2** as colourless solid (0.67 g, 1.22 mmol, 61%).

**$^1$H NMR** (400 MHz, $CDCl_3$,): δ = 7.75 (d, $^3J$ = 8.2 Hz, 4H, Ph-*H*), 7.40 (d, $^3J$ = 8.3 Hz, 4H, Ph-*H*), 6.09 (s, 4H, alkene-*H*), 3.43 (s, 6H, O-C$H_3$), 1.34 (s, 24H, C$H_3$) ppm.

**$^{11}$B NMR** (128 MHz, $CDCl_3$): δ = 30.8 ppm.

**$^{13}$C NMR** (101 MHz, $CDCl_3$) δ =146.4, 135.1, 133.4, 125.5, 83.9, 75.1, 52.10, 25.0 ppm.[2]

**M.p.:** 241 °C, lit: 250.5 °C[10]

[2] C-B signal is not visible because of the quadrupole effect of boron.

**Synthesis of Ni-[2]CPT-OMe (3)**

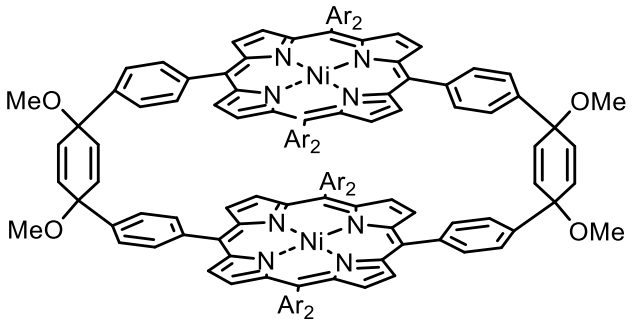


Under $N_2$, Ni-porphyrin **Ni-1-Ar$_2$** (311 mg, 0.3 mmol, 1.0 equiv), compound **2** (162 mg, 0.3 mmol, 1.0 equiv), $Cs_2CO_3$ (391 mg, 1.2 mmol, 4.0 equiv) and pyrazine (1.2 g, 15 mmol, 50 equiv) were dissolved in degassed toluene (300 mL) and the reaction solution was degassed for 30 min. $Pd(PPh_3)_4$ (64 mg, 0.06 mmol, 0.2 equiv) was added and the mixture was heated to 130°C for 1d. The reaction was concentrated and purified by column chromatography (petroleum ether/ DCM 2:1 → 1:3) to afford **Ni-[2]-CPT-OMe 3** (53 mg, 0.02 mmol, 8%) as red solid.

**$^1$H NMR** (400 MHz, $CDCl_3$): δ = 8.46 (d, $^3J$ = 4.9 Hz, 8H, Py-*H*), 8.39 (d, $^3J$ = 4.9 Hz, 8H, Py-*H*), 8.13 – 7.31 (m, 24H), 7.04 (d, $^3J$ = 8.2 Hz, 8H), 6.45 (s, 8H, alkene-*H*), 3.99 (d, $^3J$ = 5.6 Hz, 8H, O-C$H_2$), 3.66 (s, 12H, O-C$H_3$), 1.88 (m, 4H, O-CH$_2$-C*H*), 1.47 – 1.17 (m, 64H, (C$H_2$)$_n$), 1.08 – 0.73 (m, 24H, C$H_3$) ppm.

**$^{13}$C NMR** (126 MHz, $CDCl_3$): δ = 159.2, 142.1, 141.5, 141.0, 140.1, 134.6, 134.1, 133.1, 132.6, 132.3, 131.6, 128.1, 125.0, 118.3, 117.1, 113.0, 76.4, 71.3, 52.6, 38.3, 32.1, 31.7, 31.6, 31.4, 30.5, 30.4, 29.9, 29.9, 29.5, 29.3, 27.1, 23.3, 22.9, 14.3, 14.3 ppm.

**HR-MS (MALDI)**: *m/z* = calc. for $C_{152}H_{168}N_8Ni_2O_8$: 2351.17592 found: 2351.17193 [$M^+$].

**UV-vis** (DCM) $\lambda_{max}$ (ε): 416 (352500), 534 (25100) nm ($M^{-1}cm^{-1}$).

**Synthesis of [5,15-bis(4-((2-butyloctyl)oxy)phenyl)-10,20-diphenylporphyrin]nickel(II) (4)**

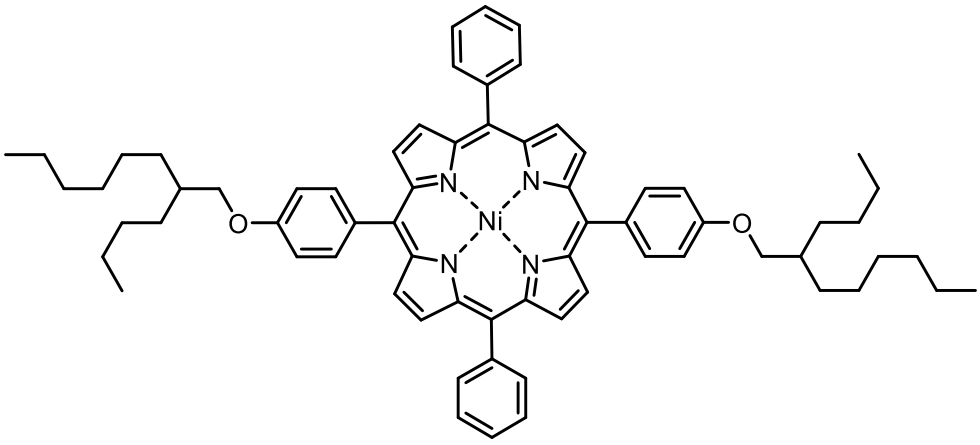


Under $N_2$, Ni-porphyrin **Ni-1-Ar$_2$** (100 mg, 0.09 mmol, 1.0 equiv), phenylboronic acid pinacol ester (55 mg, 0.27 mmol, 3.0 equiv), $Cs_2CO_3$ (205 mg, 0.63 mmol, 7.0 equiv) were dissolved in toluene (5 mL) and DMF (1 mL) and the reaction solution was degassed for 30 min. $Pd(PPh_3)_4$ (10 mg, 0.01 mmol, 0.1 equiv) was added and the mixture was heated to 60°C for 1d. The reaction was concentrated and purified by column chromatography (petroleum ether/ DCM 5:1) to afford Ni(II)porphyrin **4** (54 mg, 0.052 mmol, 58%) as red solid.

**$^1$H NMR** (400 MHz, $CDCl_3$): δ = 8.79 (d, $^3J$ = 5.0 Hz, 4H, Py-*H*), 8.73 (d, $^3J$ = 4.9 Hz, 4H, Py-*H*), 8.01 (d, $^3J$ = 7.5 Hz, 4H, Ph-*H*), 7.90 (d, $^3J$ = 8.4 Hz, 4H, Ph-*H*), 7.73 – 7.63 (m, 6H, Ph-*H*), 7.20 (d, $^3J$ = 8.6 Hz, 4H, Ph-*H*), 4.07 (d, $^3J$ = 5.7 Hz, 4H, O-$CH_2$), 2.10 – 1.81 (m, 2H, C*H*), 1.50 – 1.28 (m, 32H, $(CH_2)_n$), 0.98 (t, $^3J$ = 6.8 Hz, 6H, $CH_3$), 0.92 (t, $^3J$ = 6.8 Hz, 3H, $CH_3$) ppm.

**$^{13}$C NMR** (101z MHz, $CDCl_3$): δ = 159.4, 143.2, 142.7, 141.1, 134.9, 133.9, 133.1, 132.4, 132.1, 127.8, 127.0, 119.0, 118.9, 113.1, 71.4, 38.3, 32.1, 31.7, 31.4, 29.9, 29.4, 27.1, 23.3, 22.9, 14.3, 14.3.ppm.

**HR-MS (MALDI)**: *m/z* = calc. for $C_{68}H_{76}N_4NiO_2$: 1038.5322 found: 1038.52971 [$M^+$].

**UV-vis** (DCM) $\lambda_{max}$ (ε): 417 (257000), 530 (18200) nm ($M^{-1}cm^{-1}$).

# 5. Electrocatalytic Studies

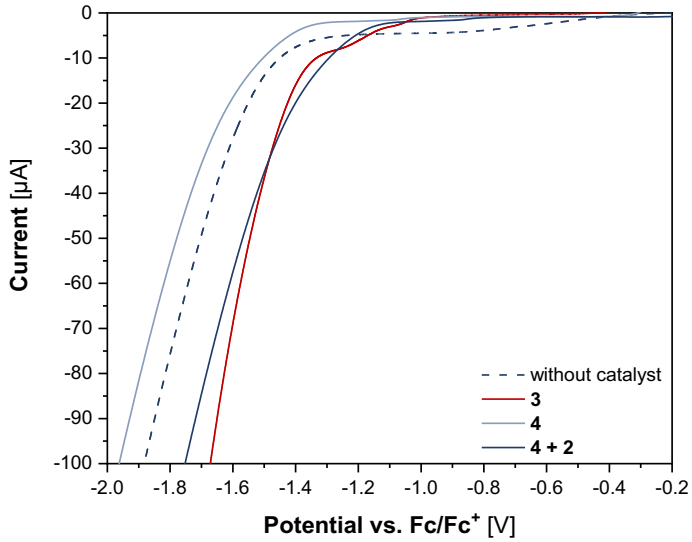


**Figure S7**: Linear sweep voltammograms in the presence of acetic acid (HOAc, 0.1 M) in dichloromethane with 0.1 M [$^n$Bu$_4$N][PF$_6$] at 100 mV s$^{-1}$ without (dotted black) and with complexes **3** (red), complex **4** (light blue) as well as **4** and **2** (dark blue), respectively.

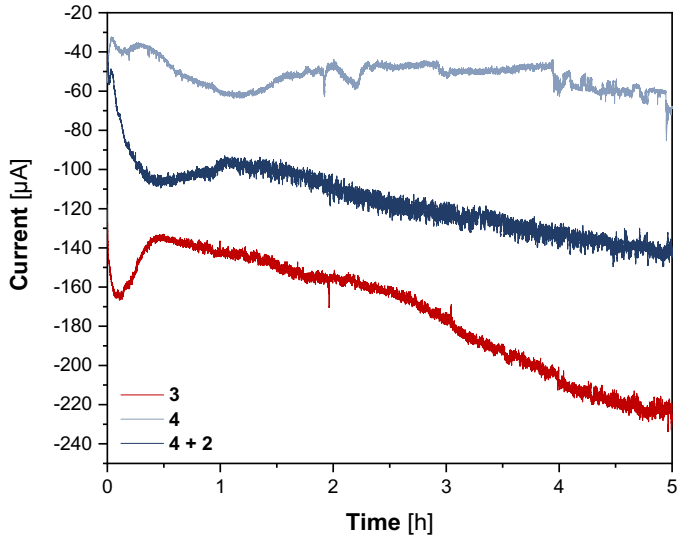


**Figure S8**: Controlled potential coulometry of 1 mM complex solutions in the presence of 0.1 M acetic acid with 0.1 M [$^n$Bu$_4$N][PF$_6$] at a defined potential for 5 h. The potential during electrolysis was held at -1.87 V vs. Fc/Fc$^+$ for **3** (red), at -1.90 V vs. Fc/Fc$^+$ for complex **4** (light blue) as well as at -1.94 V vs Fc/Fc$^+$ for **4** and **2**.

**Table S1**: Quantification of the electrocatalytically generated $H_2$ by GC-MS.

| | **E vs. $Fc/Fc^+$ [V]** | **time [h]** | **$H_2$ [ppm]** | **$FE_{H2}$ [%]** |
|---|---|---|---|---|
| **3** | -1.87 | 1 | 12 279 | 87 |
| | | 2 | 21 091 | 90 |
| | | 3 | 30 826 | 95 |
| | | 4 | 36 092 | 86 |
| | | 5 | 49 421 | 93 |
| **4** | -1.90 | 1 | 1 538 | 80 |
| | | 2 | 3 560 | 85 |
| | | 3 | 4 276 | 70 |
| | | 4 | 5 266 | 65 |
| | | 5 | 7 032 | 66 |
| **4 + 2** | -1.94 | 1 | 4 540 | 85 |
| | | 2 | 8 313 | 77 |
| | | 3 | 12 768 | 84 |
| | | 4 | 16 856 | 93 |
| | | 5 | 22 210 | 94 |

## 6. DFT Calculations

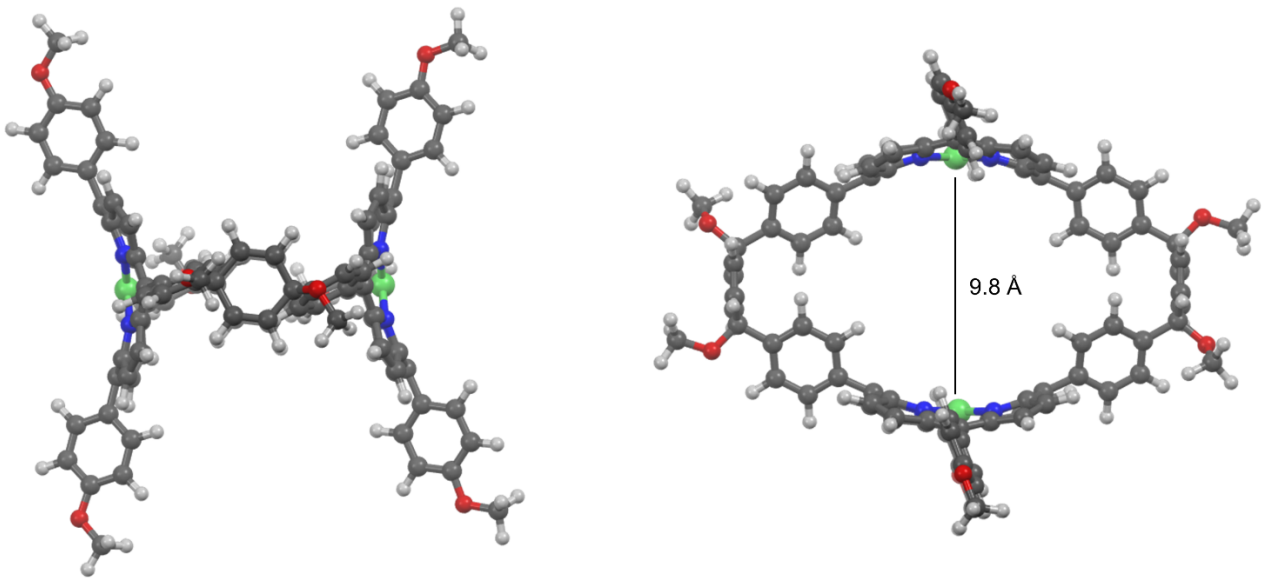


**Figure S9:** Optimized Structures (B3LYP/6-31G(d)) of Ni-[2]CPT-OMe **3**.

The optimized structure from DFT calculations can be found on figshare:

Schwer, Fabian; von Delius, Max (2020): Ni-2-CPT-OMe_B3LYP-631Gd.xyz. figshare. Dataset.

https://doi.org/10.6084/m9.figshare.13032722.v1

# 7. Spectra

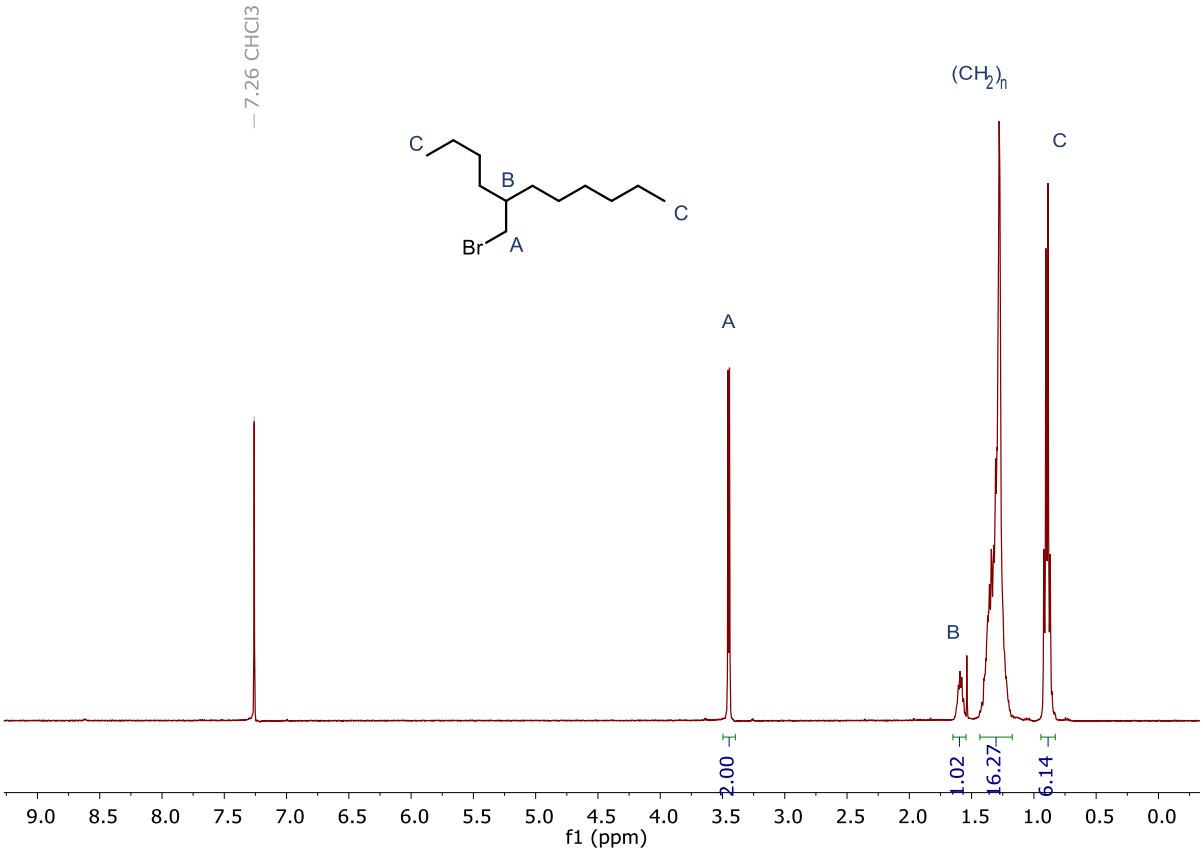


**Figure S10**:[1]H NMR (400 MHz, $CDCl_3$) of compound **S1**.

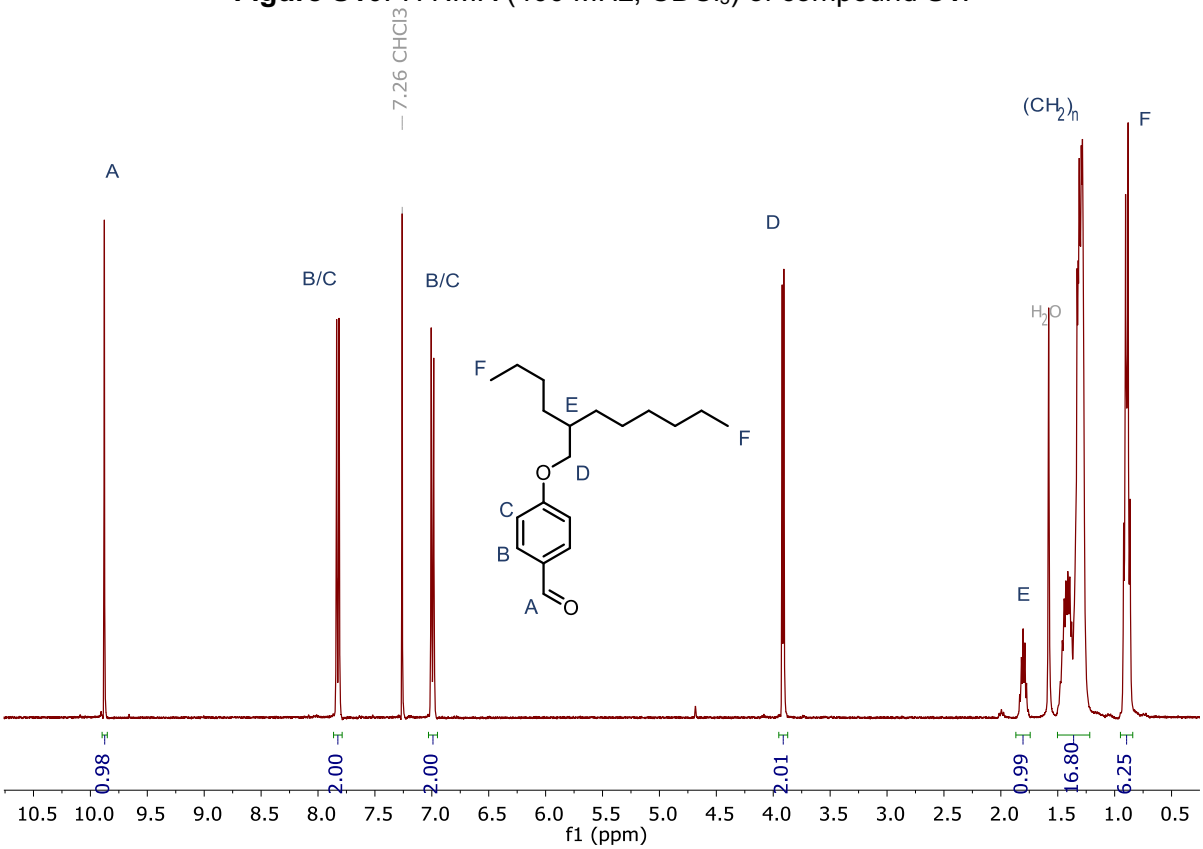


**Figure S11**: [1]H NMR (400 MHz, $CDCl_3$) of compound **S2**.

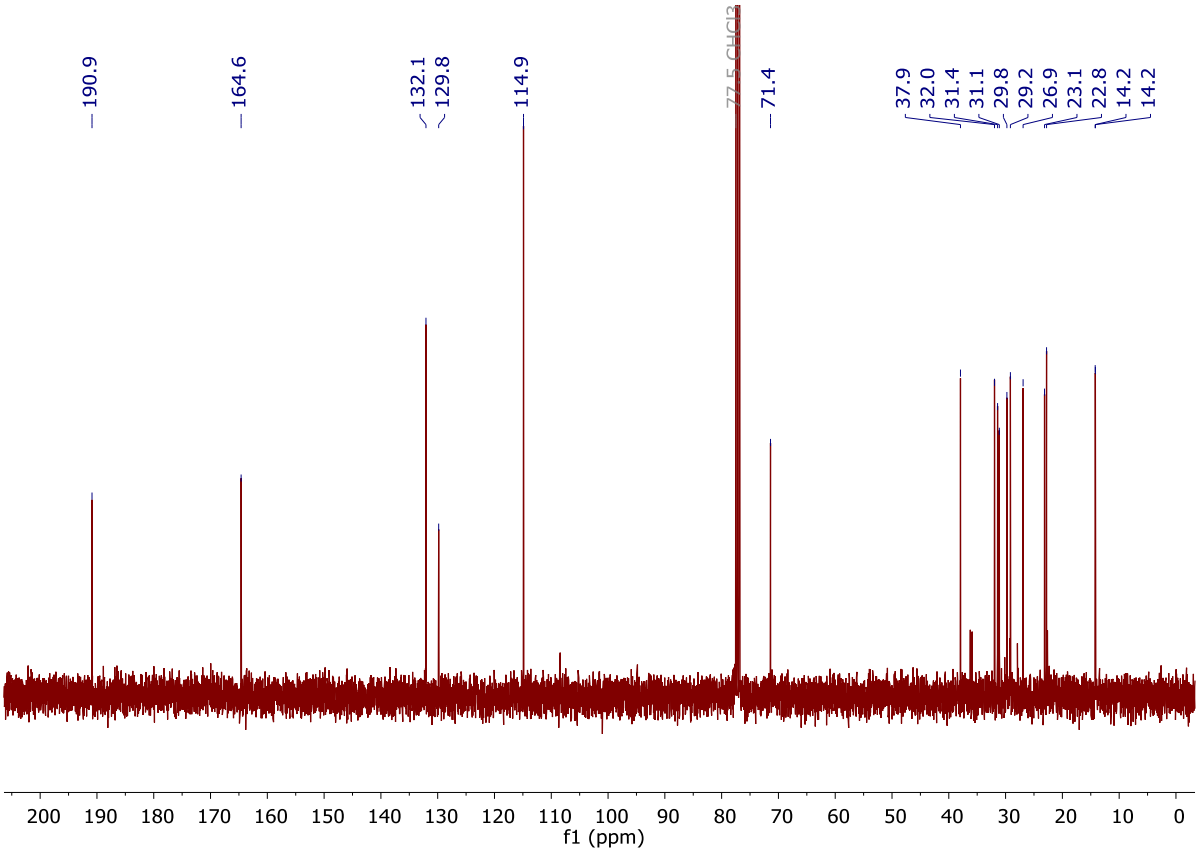


**Figure S12**: $^{13}C$ NMR (101 MHz, $CDCl_3$) of compound **S2**.

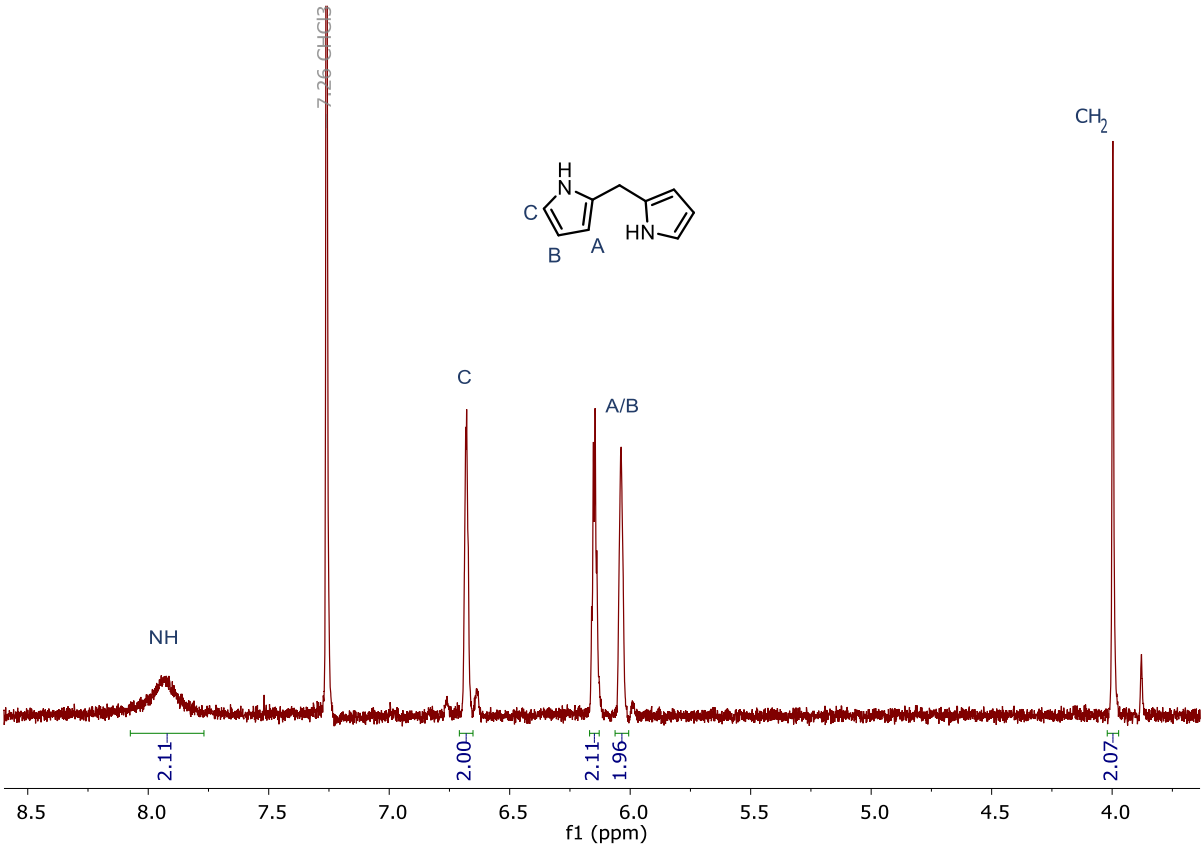


**Figure S13**: $^{1}H$ NMR (400 MHz, $CDCl_3$) of compound **S3**.

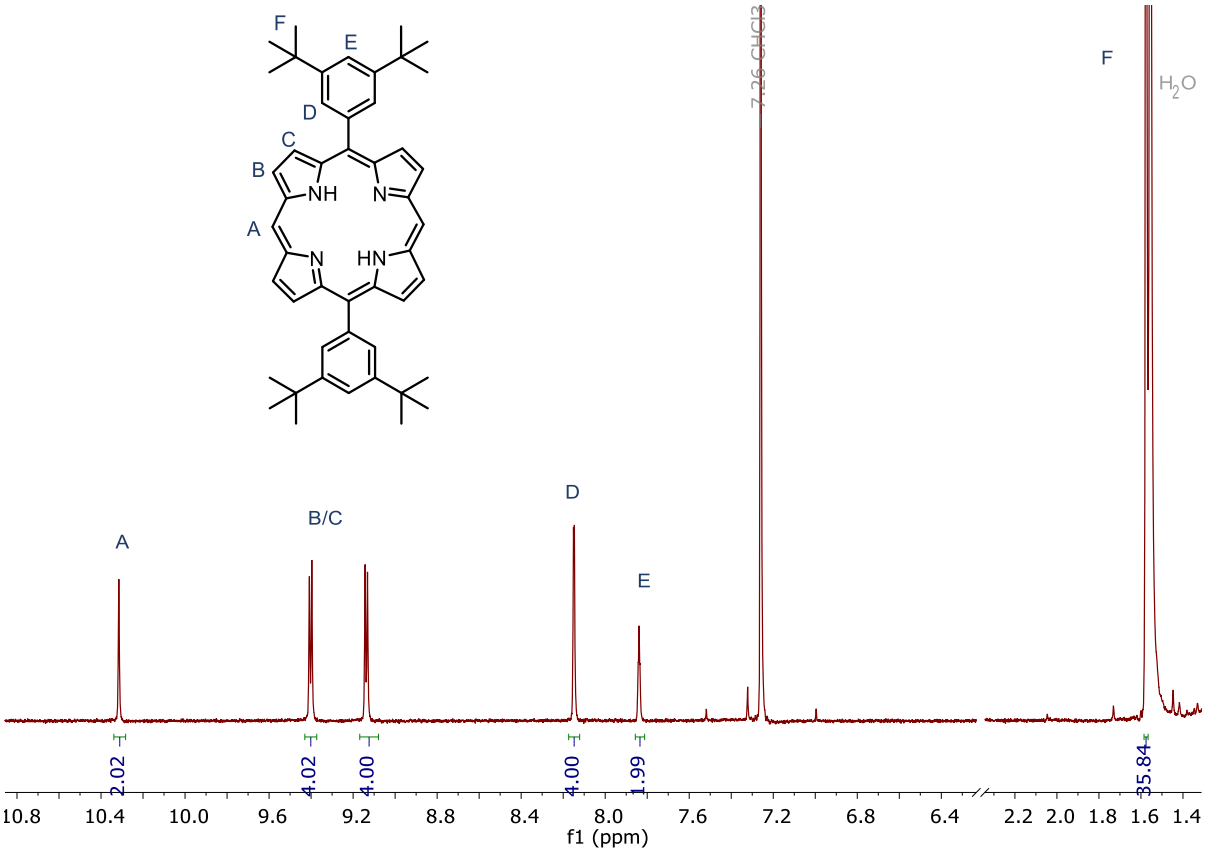


**Figure S14**: $^{1}$H NMR (400 MHz, $CDCl_3$) of compound **S4-Ar$_1$**.

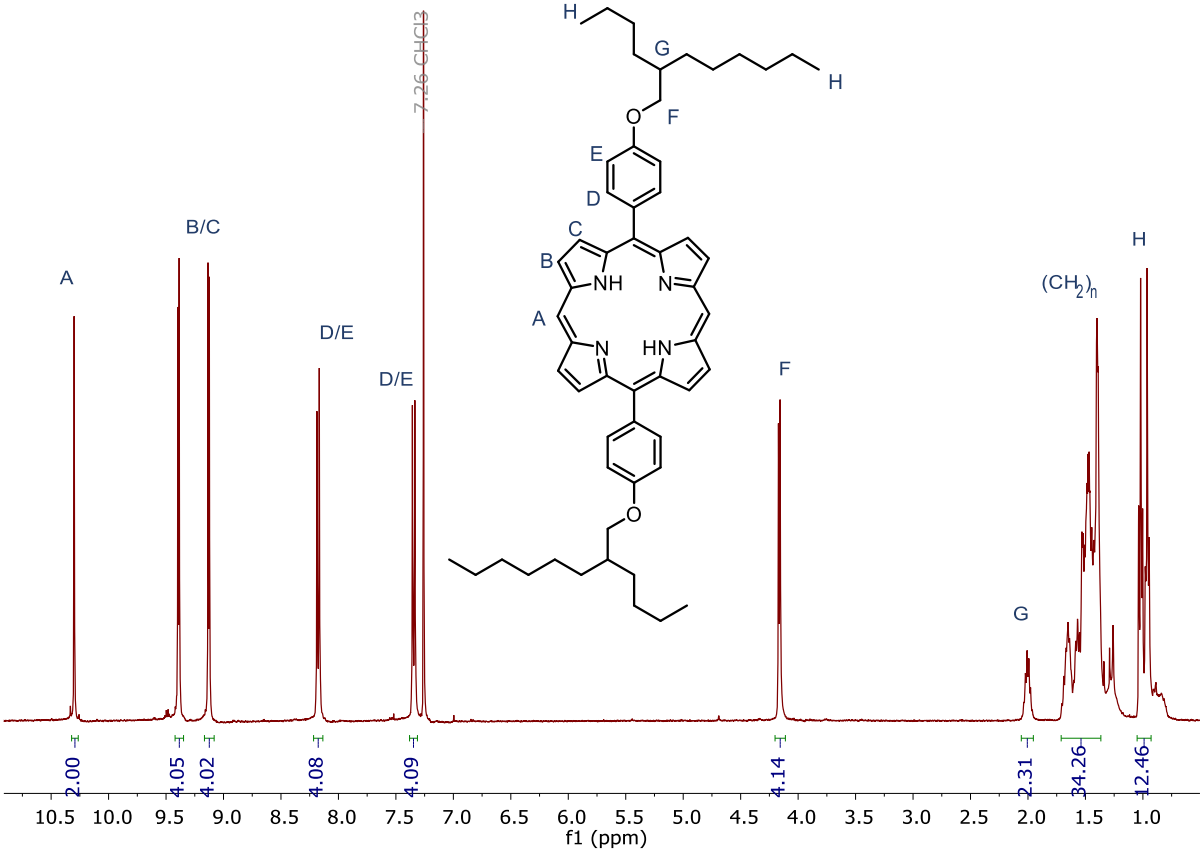


**Figure S15**: $^{1}$H NMR (400 MHz, $CDCl_3$) of porphyrin **S4-Ar$_2$**.

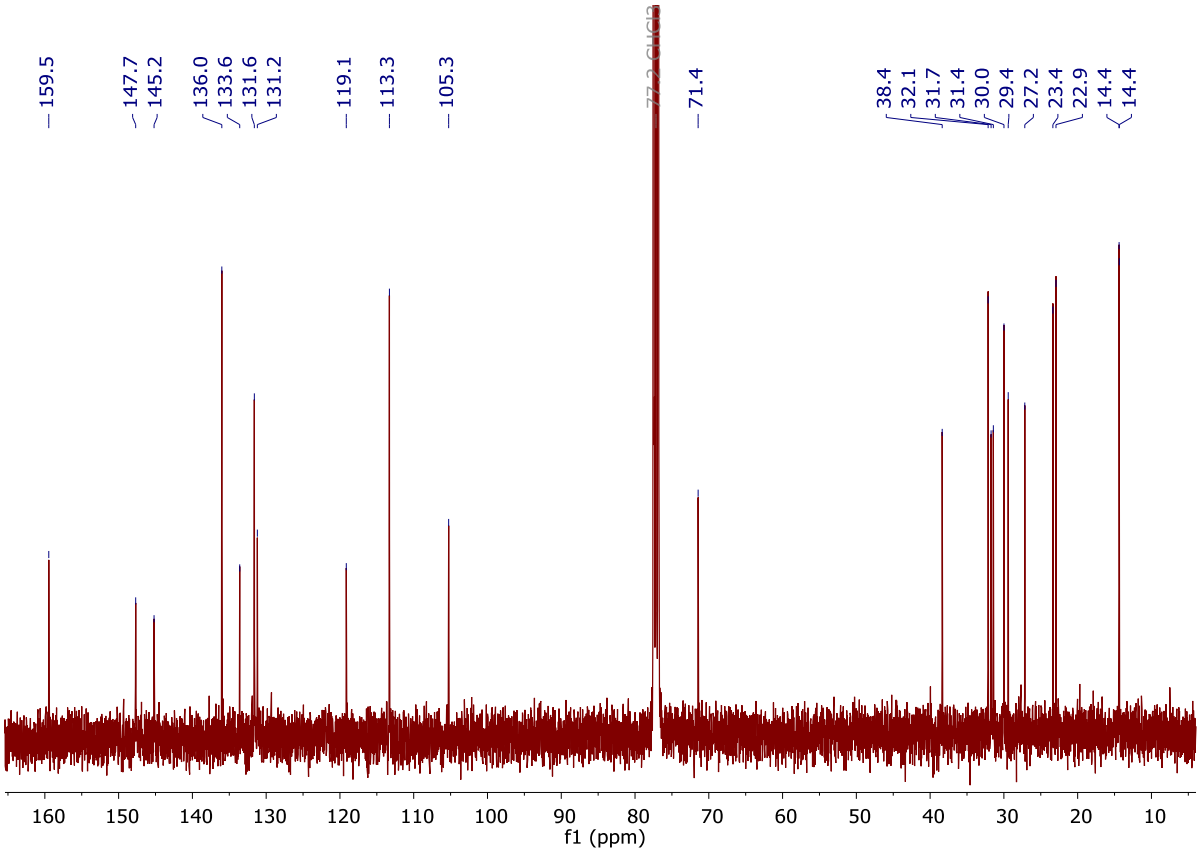


**Figure S16**: $^{13}C$ NMR (101 MHz, $CDCl_3$) of porphyrin **S4-Ar$_2$**.

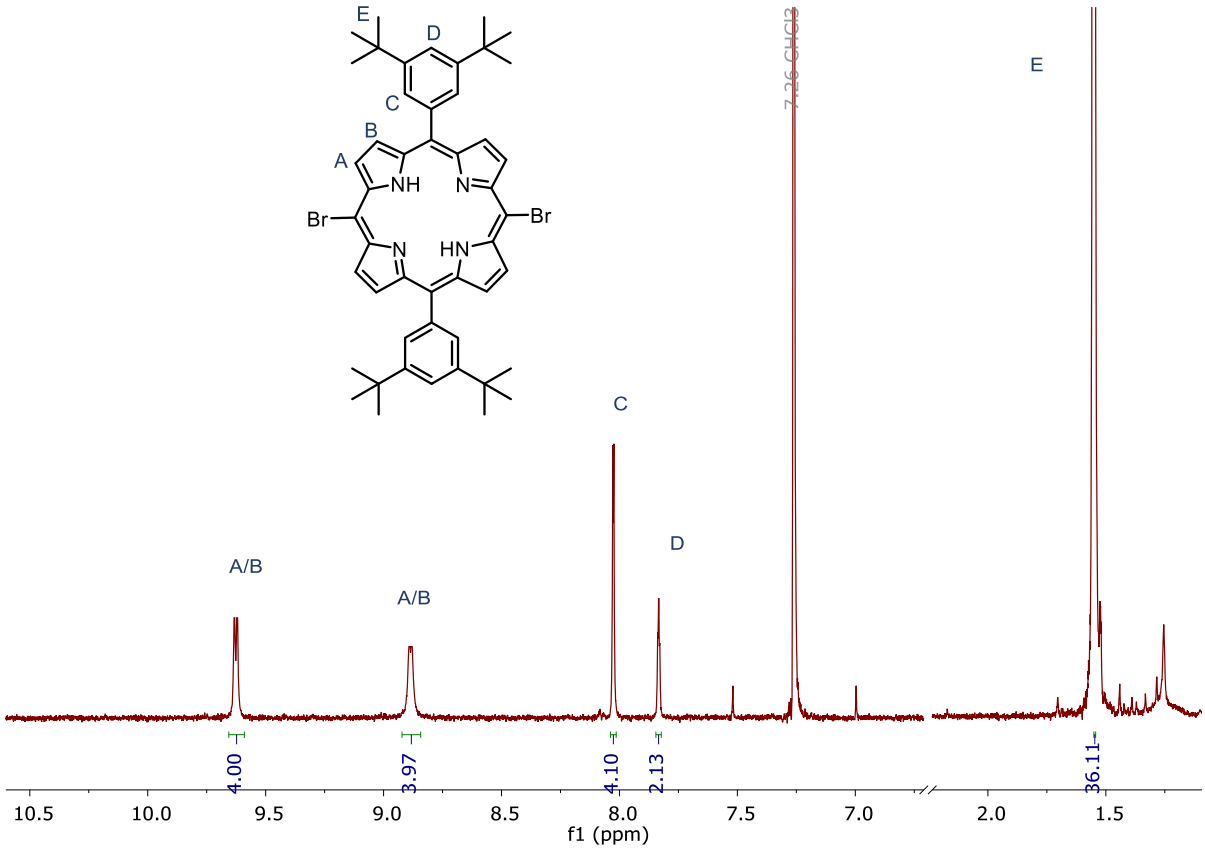


**Figure S17**: $^{1}H$ NMR (400 MHz, $CDCl_3$) of porphyrin **S5-Ar$_1$**.

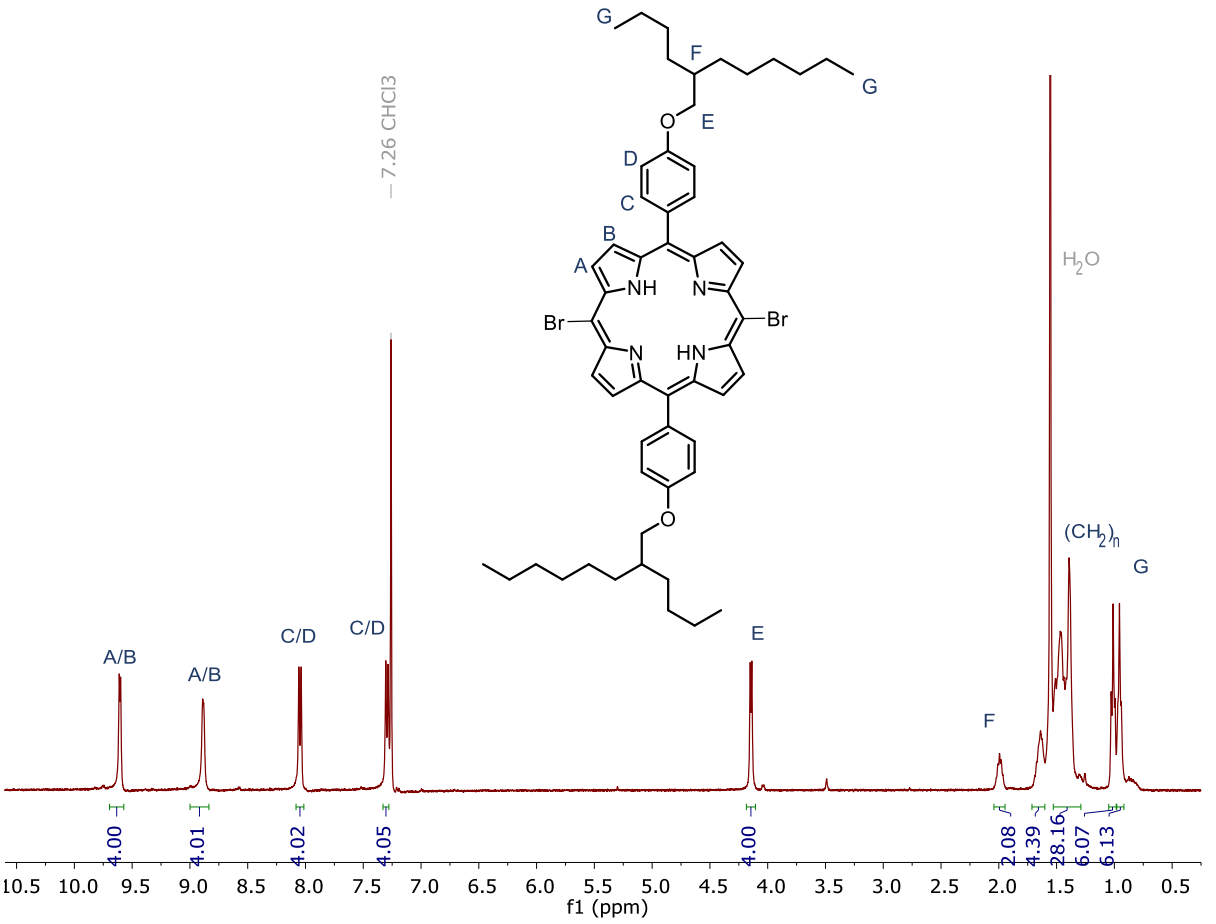


**Figure S18**: $^{1}$H NMR (400 MHz, $CDCl_3$) of porphyrin **S5-Ar$_2$**.

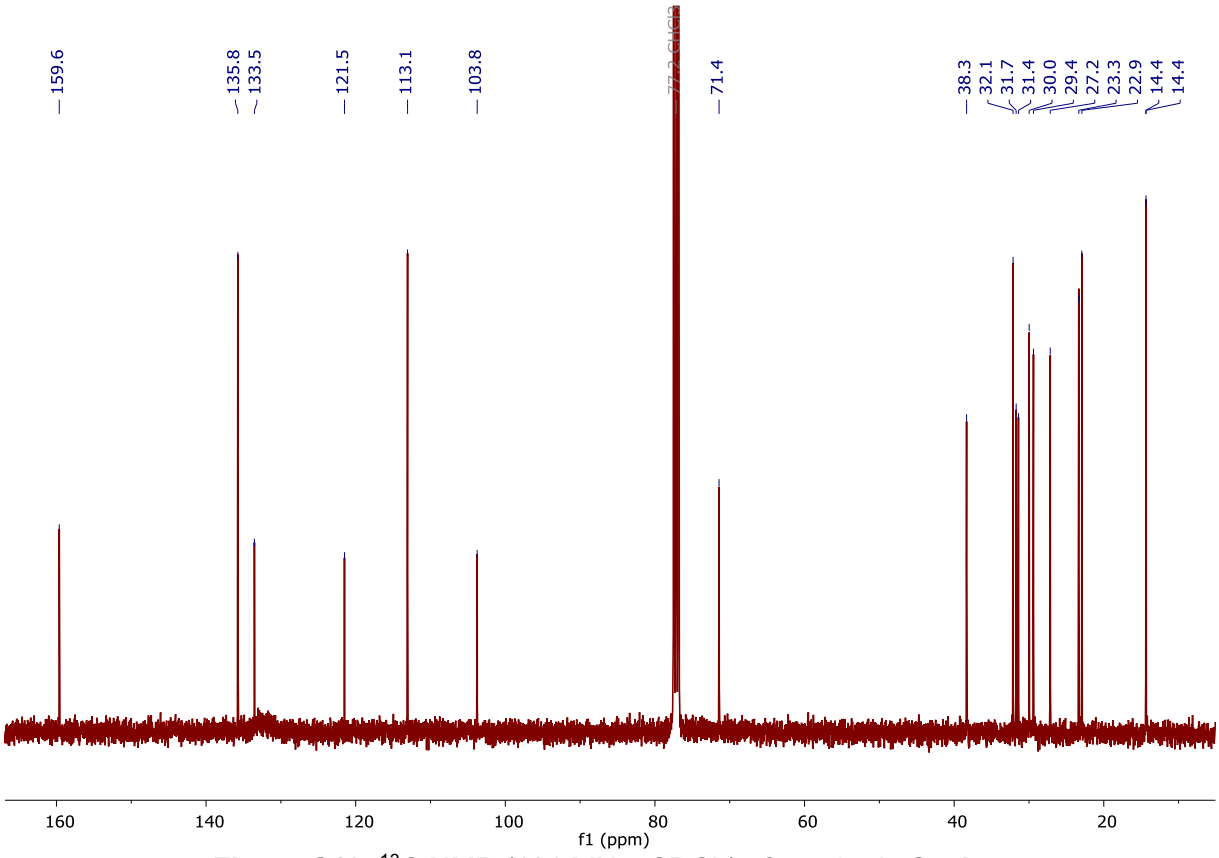


**Figure S19**: $^{13}$C NMR (101 MHz, $CDCl_3$) of porphyrin **S5-Ar$_2$**.

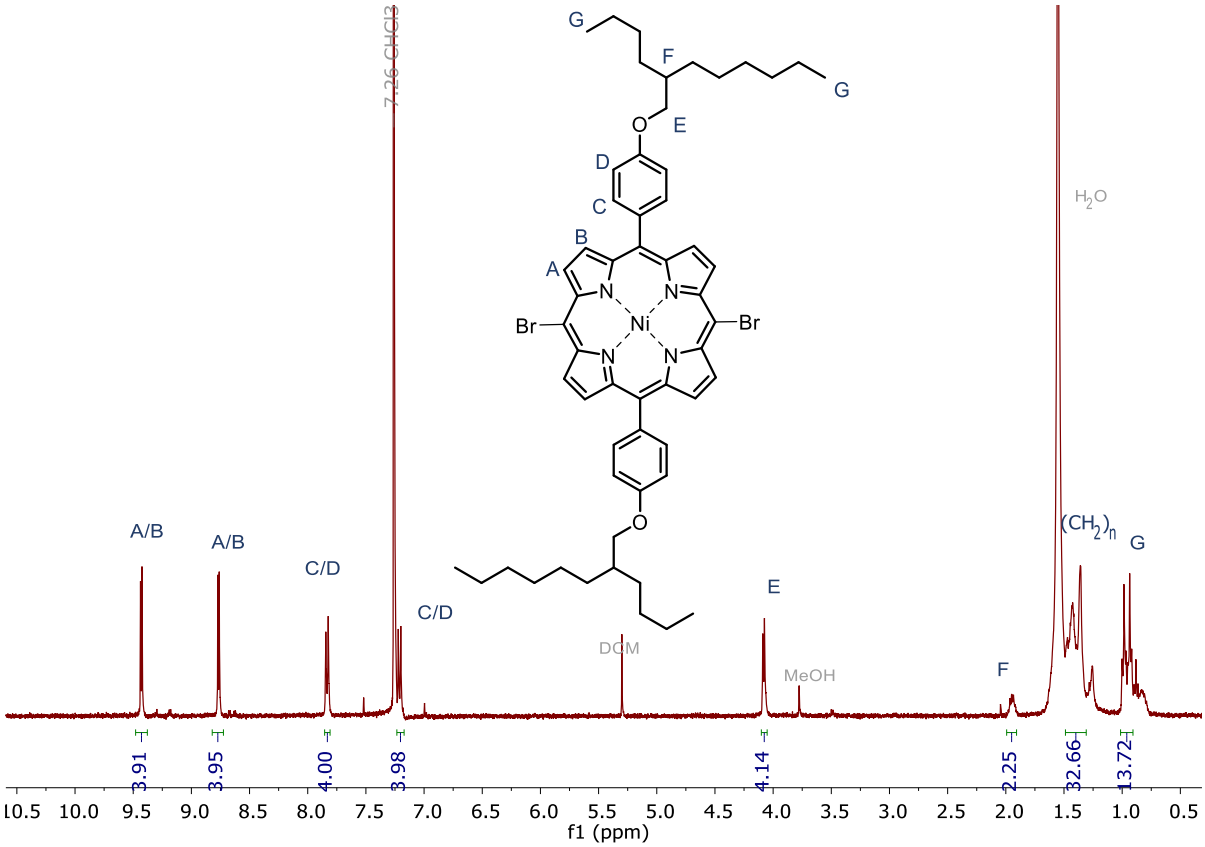


**Figure S20**: $^{1}$H NMR (400 MHz, $CDCl_3$) of porphyrin **Ni-1-Ar$_2$**.

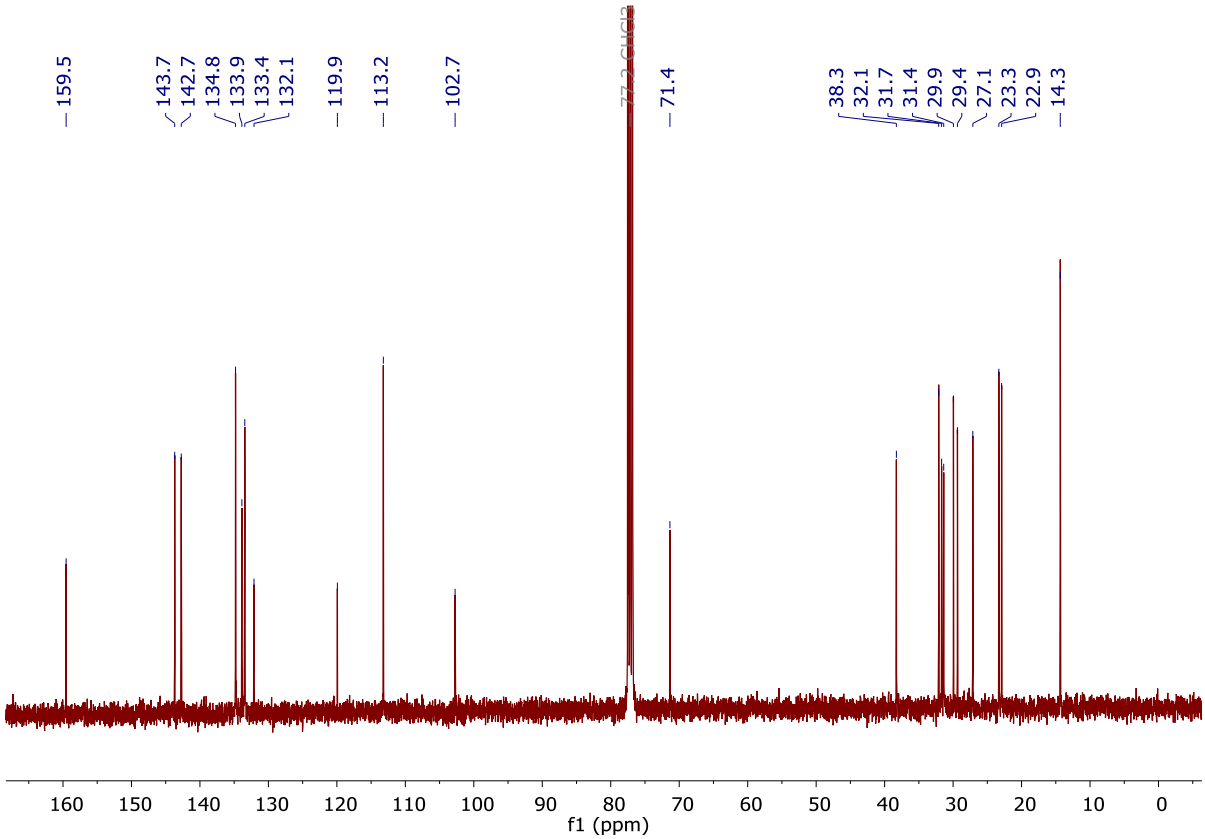


**Figure S21**:$^{13}$C NMR (101 MHz, $CDCl_3$) of porphyrin **Ni-1-Ar$_2$**.

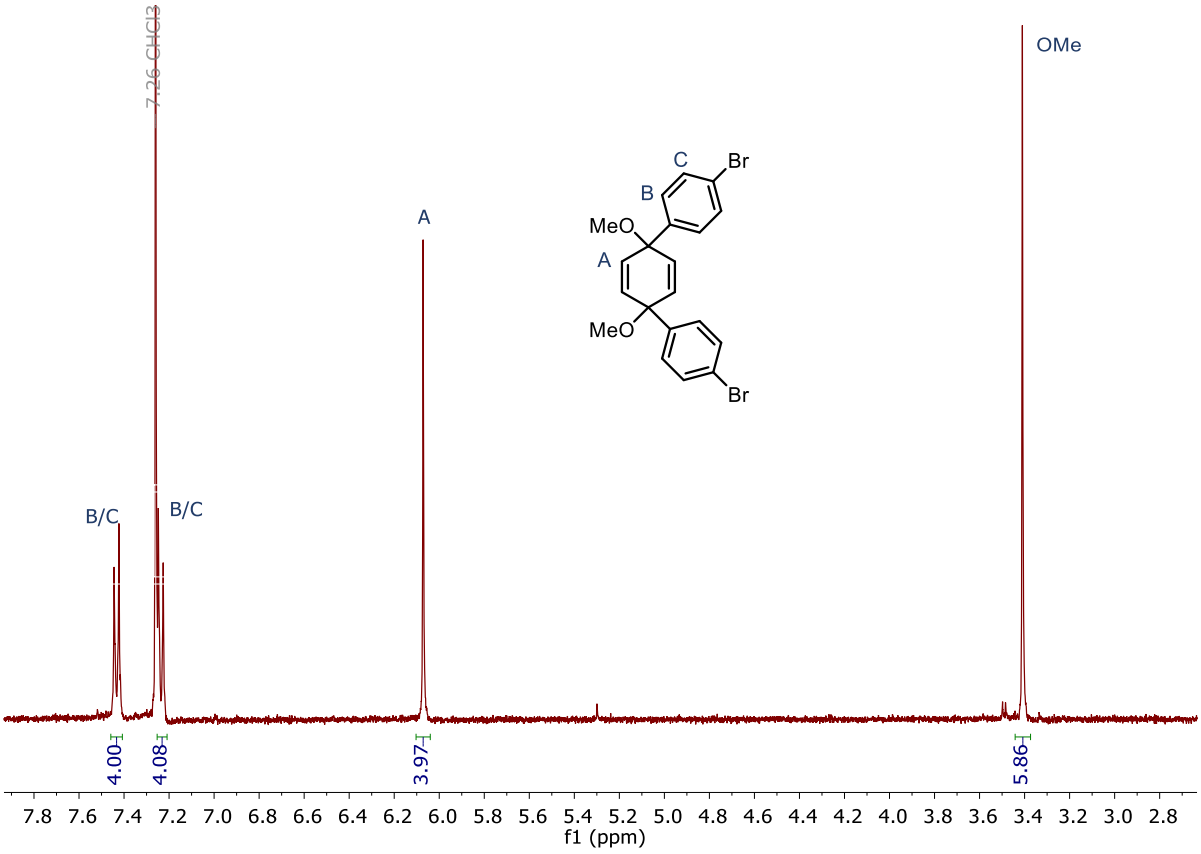


**Figure S22**: $^{1}$H NMR (400 MHz, $CDCl_3$) of compound **S7**.

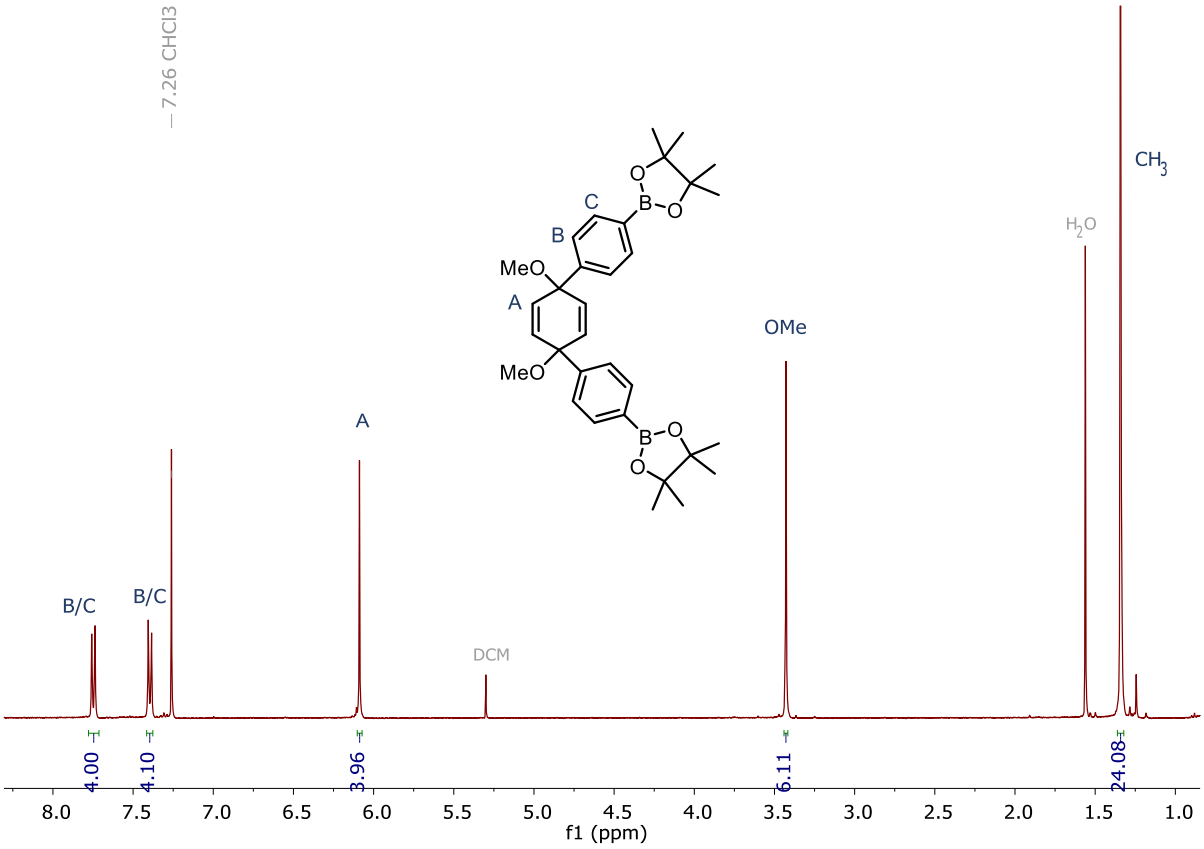


**Figure S23**: $^{1}$H NMR (400 MHz, $CDCl_3$) of compound **2.**

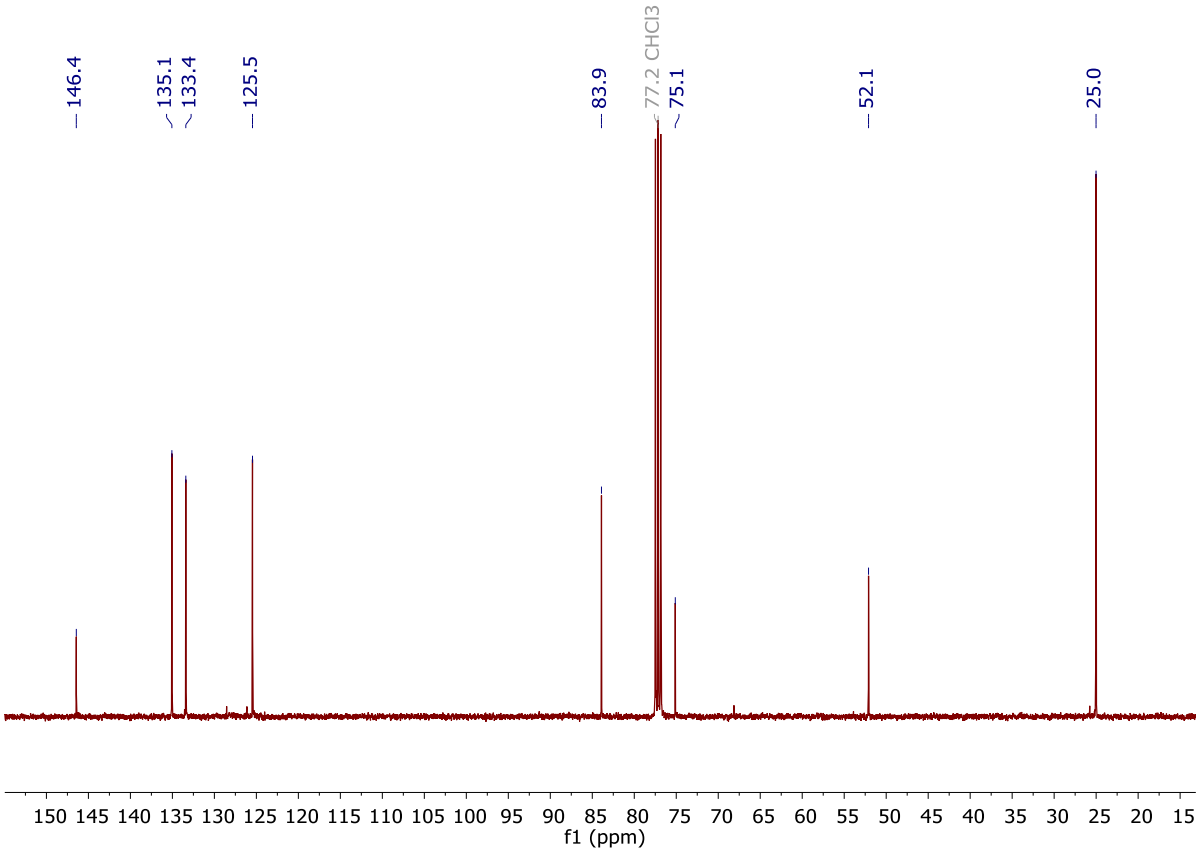


**Figure S24**: $^{13}C$ NMR (101 MHz, $CDCl_3$) of compound **2**.

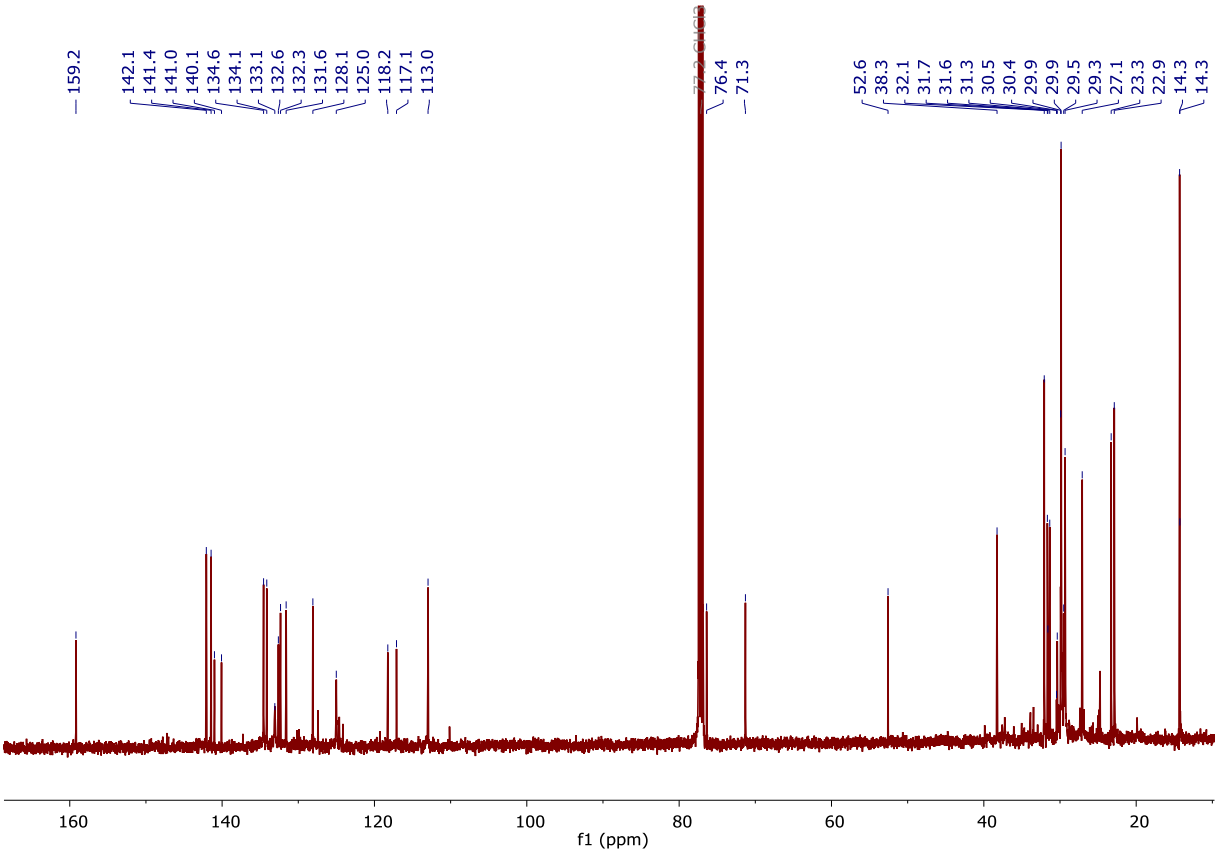


**Figure S25**:$^{13}C$ NMR (126 MHz, $CDCl_3$) of **Ni-[2]CPT-OMe 3.**

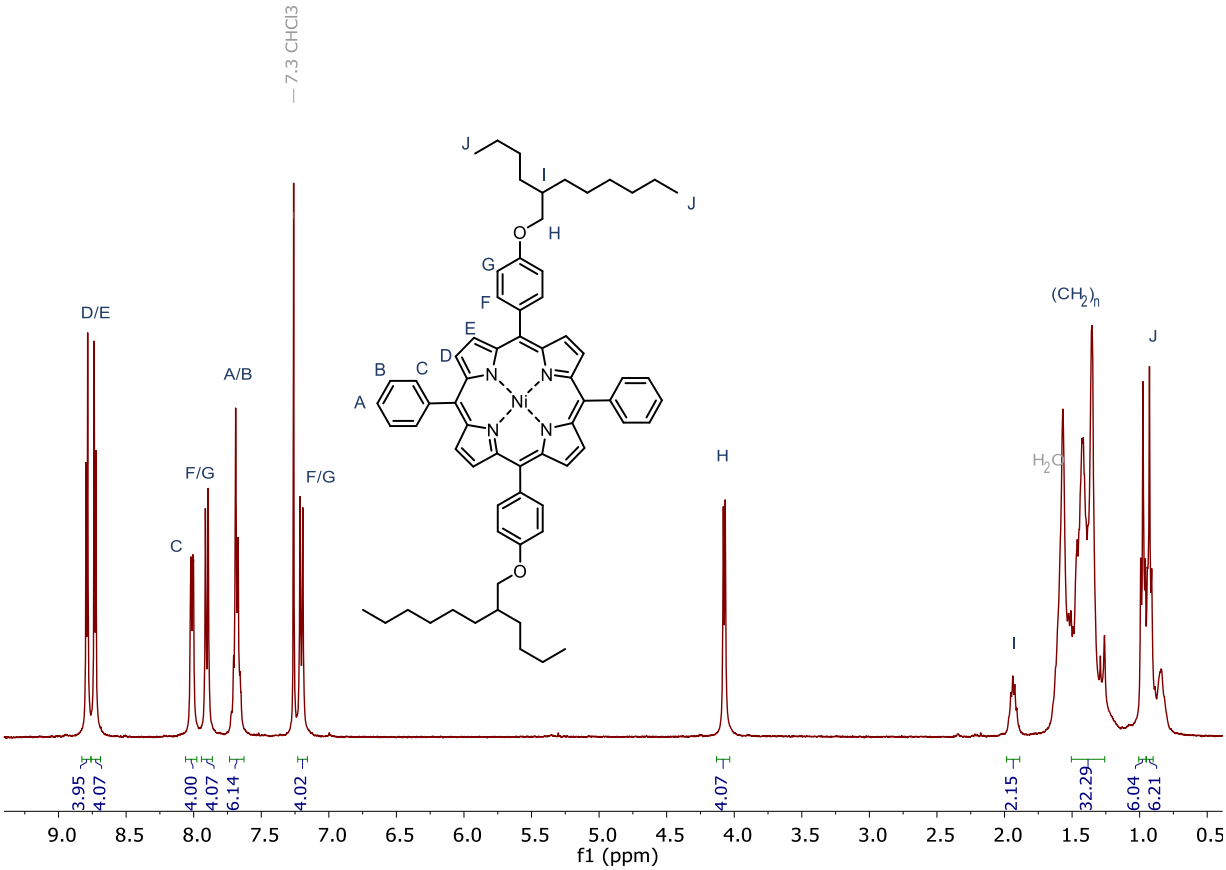


**Figure S26**: $^{1}$H NMR (400 MHz, $CDCl_3$) of compound **4.**

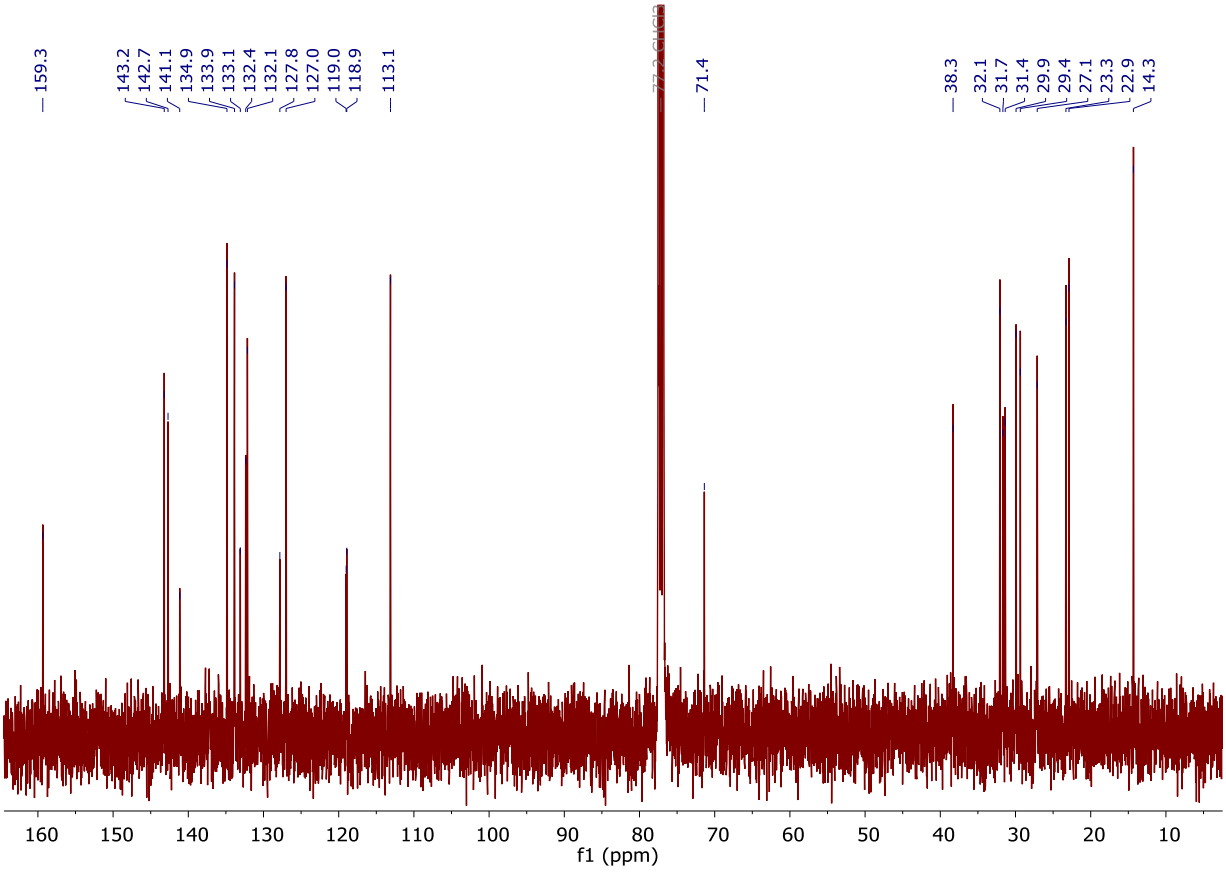


**Figure S27**: $^{13}$C NMR (101 MHz, $CDCl_3$) of compound **2**.

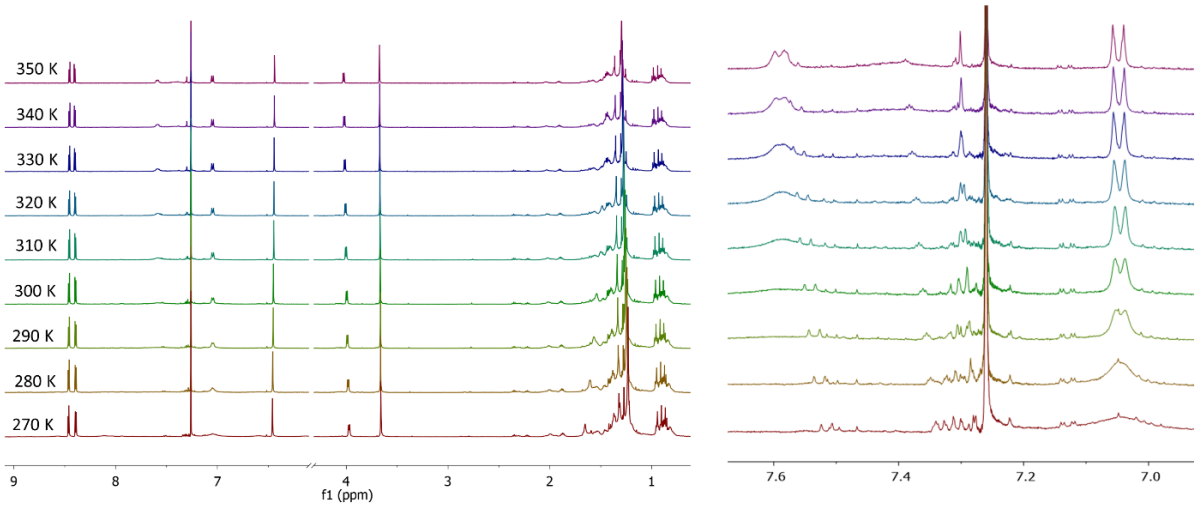


**Figure S28**: Variable temperature $^{1}H$ NMR (500 MHz, $CDCl_3$) of **Ni-[2]CPT-OMe 3**.

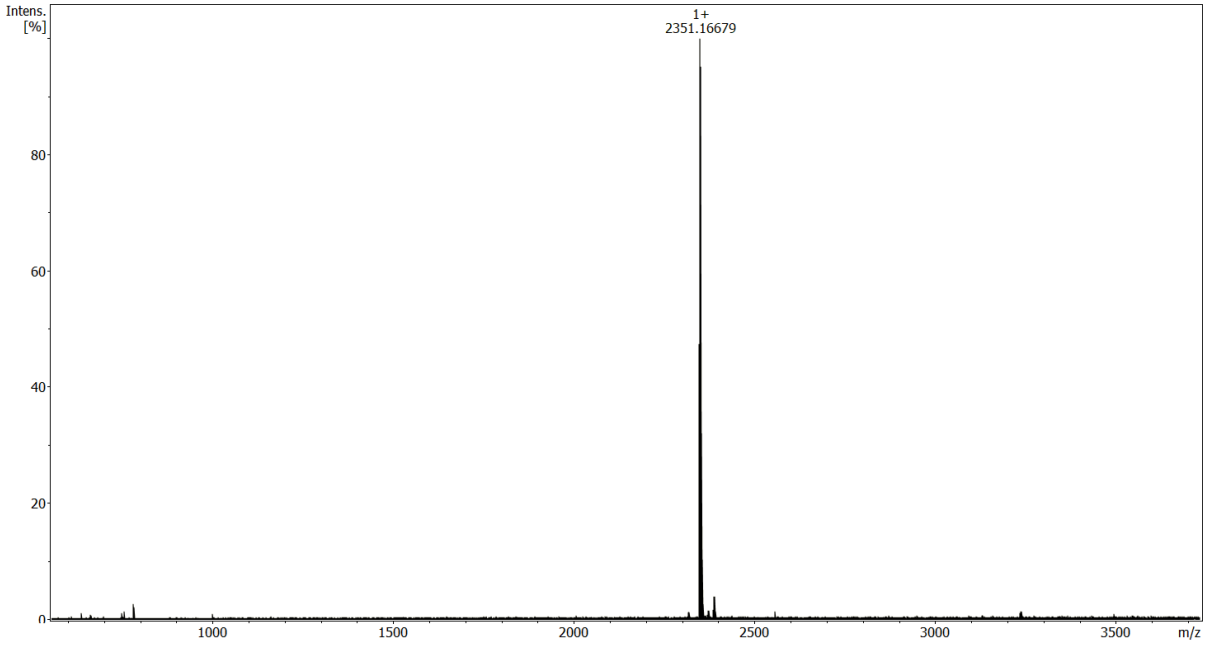


**Figure S29**: HRMS (MALDI, matrix: DCTB) of **Ni-[2]CPT-OMe 3**.

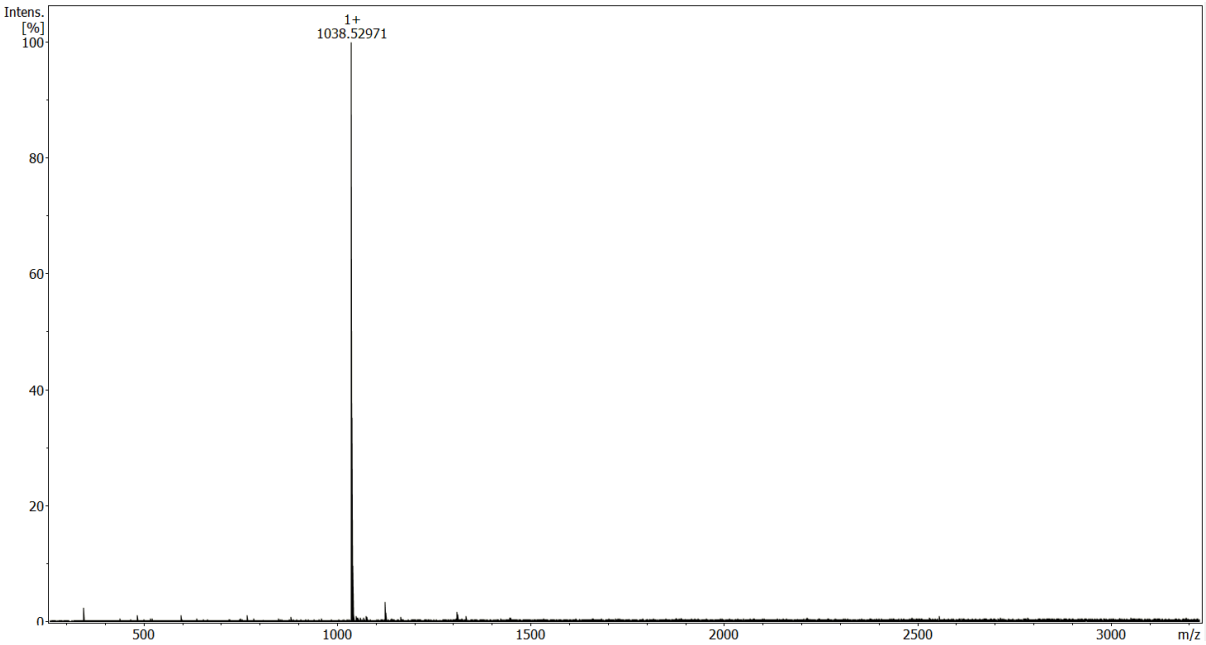


**Figure S30**: HRMS (MALDI, matrix: DCTB) of Ni(II)porphyrin **4**.

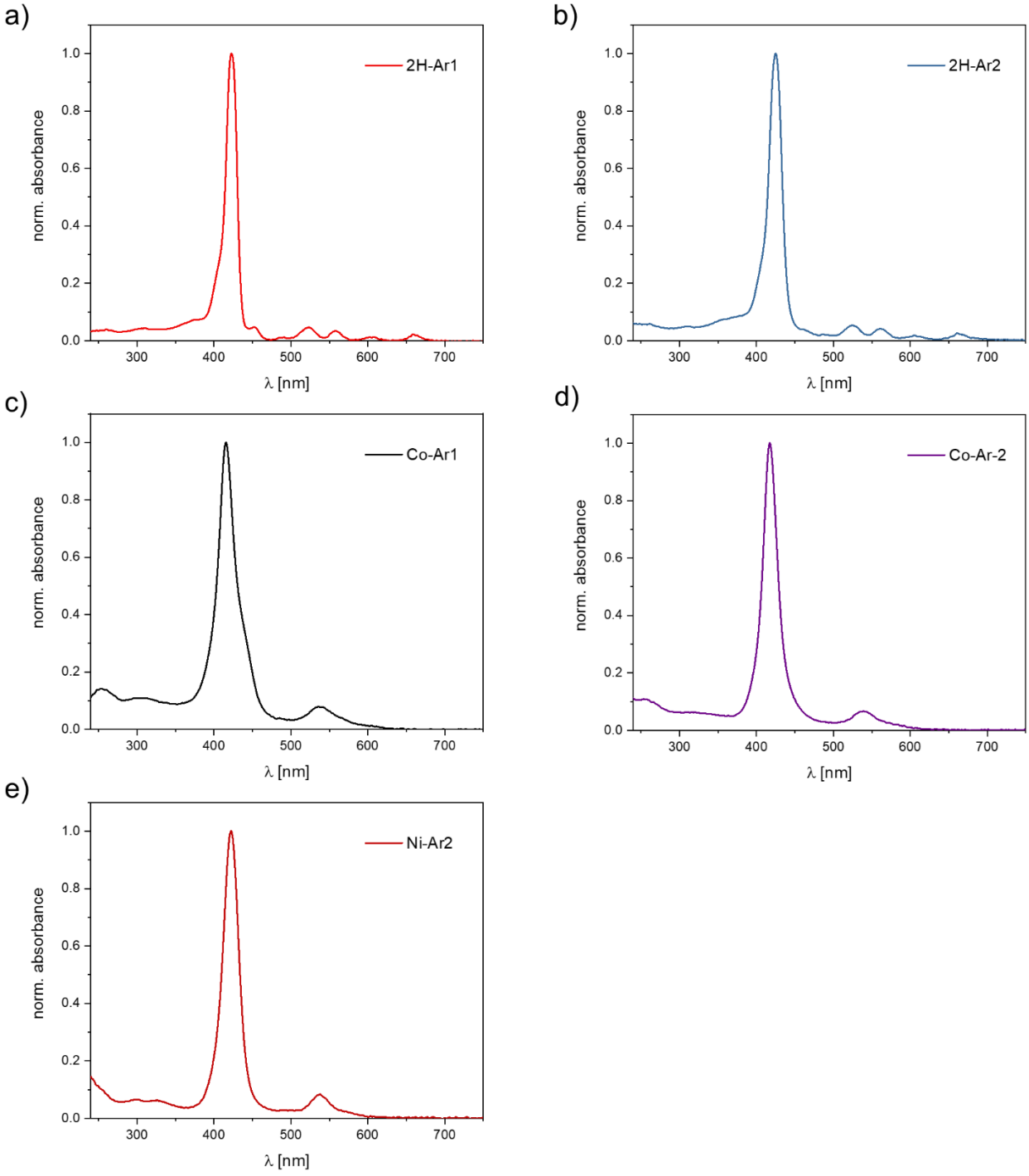


**Figure S31**: Absorption spectra in DCM. a) free-base porphyrin **S5-Ar$_1$**. b) free-base porphyrin **S5-Ar$_2$**. c) cobalt(II)porphyrin **Co-1-Ar$_1$**. d) cobalt(II)porphyrin **Co-1-Ar$_2$**. e) nickel(II)porphyrin **Ni-1-Ar$_2$**.

## 8. References


1 G. E. S. M. J. Frisch, G. W. Trucks, H. B. Schlegel, V. B. M. A. Robb, J. R. Cheeseman, G. Scalmani, A. V. M. G. A. Petersson, H. Nakatsuji, X. Li, M. Caricato, H. P. H. J. Bloino, B. G. Janesko, R. Gomperts, B. Mennucci, D. W.-Y. J. V. Ortiz, A. F. Izmaylov, J. L. Sonnenberg, A. P. F. Ding, F. Lipparini, F. Egidi, J. Goings, B. Peng, N. R. T. Henderson, D. Ranasinghe, V. G. Zakrzewski, J. Gao, R. F. G. Zheng, W. Liang, M. Hada, M. Ehara, K. Toyota, H. N. J. Hasegawa, M. Ishida, T. Nakajima, Y. Honda, O. Kitao, J. E. P. T. Vreven, K. Throssell, J. A. Montgomery, Jr., K. N. K. F. Ogliaro, M. J. Bearpark, J. J. Heyd, E. N. Brothers, J. N. V. N. Staroverov, T. A. Keith, R. Kobayashi, S. S. I. K. Raghavachari, A. P. Rendell, J. C. Burant, R. C. J. Tomasi, M. Cossi, J. M. Millam, M. Klene, C. Adamo, O. F. J. W. Ochterski, R. L. Martin, K. Morokuma and D. J. F. J. B. Foresman, Gaussian, Inc., Wallingford CT, 2019.

2 Y. Xu, S. Gsänger, M. B. Minameyer, I. Imaz, D. Maspoch, O. Shyshov, F. Schwer, X. Ribas, T. Drewello, B. Meyer and M. Von Delius, *J. Am. Chem. Soc.*, 2019, **141**, 18500–18507.

3 S. L. Fronk, M. Wang, M. Ford, J. Coughlin, C. K. Mai and G. C. Bazan, *Chem. Sci.*, 2016, **7**, 5313–5321.

4 A. Shanavas, S. Sathiyaraj, A. Chandramohan, T. Narasimhaswamy and A. Sultan Nasar, *J. Mol. Struct.*, 2013, **1038**, 126–133.

5 A. J. F. N. Sobral, N. G. C. L. Rebanda, M. Da Silva, S. H. Lampreia, M. Ramos Silva, A. Matos Beja, J. A. Paixão and A. M. D. A. Rocha Gonsalves, *Tetrahedron Lett.*, 2003, **44**, 3971–3973.

6 J. S. Manka and D. S. Lawrence, *Tetrahedron*, 1989, **30**, 6989–6992.

7 S. K. Albert, M. Golla, H. V. P. Thelu, N. Krishnan, P. Deepak and R. Varghese, *Org. Biomol. Chem.*, 2016, **14**, 6960–6969.

8 M. J. Plater, S. Aiken and G. Bourhill, *Tetrahedron*, 2002, **58**, 2405–2413.

9 T. S. Balaban, R. Goddard, M. Linke-Schaetzel and J. M. Lehn, *J. Am. Chem. Soc.*, 2003, **125**, 4233–4239.

10 A. Abdulkarim, F. Hinkel, D. Jänsch, J. Freudenberg, F. E. Golling and K. Müllen,

*J. Am. Chem. Soc.*, 2016, **138**, 16208–16211.